LUND UNIVERSITY

Thermoelectric Effects and Single Electron Sources in Mesoscopic Transport; a Scattering Approach

Kheradsoud, Sara

2019

Document Version:
Publisher's PDF, also known as Version of record

Thermoelectric Effects and Single Electron Sources in Mesoscopic Transport; a Scattering Approach

Thermoelectric Effects and Single Electron Sources in Mesoscopic Transport; a Scattering Approach

by Sara Kheradsoud

LUND
UNIVERSITY

Thesis for the degree of Doctor of Philosophy in Engineering
Thesis advisors: Assoc. Prof. Peter Samuelsson, Assoc. Prof. Claudio Verdozzi
Faculty opponent: Dr. Robert S. Whitney

To be presented, with the permission of the Faculty of Science of Lund University, for public criticism in the Rydberg lecture hall (Rydbergsalen) at the Department of Physics on Friday, the 15th of November 2019 at 09:00.

Organization
LUND UNIVERSITY

Department of Physics
Box 118
SE–221 00 LUND
Sweden

Document name
DOCTORAL DISSERTATION

Date of disputation
2019-11-15

Sponsoring organization

Author(s)
Sara Kheradsoud

Title and subtitle
Thermoelectric Effects and Single Electron Sources in Mesoscopic Transport; a Scattering Approach

Abstract
This thesis concerns the theoretical analysis of thermoelectric transport properties and single electron sources in mesoscopic conductors. We propose two types of thermoelectric heat engines and analyze them with the help of performance quantifiers. We also investigate and compare the properties of different single electron sources, focusing on their coupled charge and energy transport. As a common denominator, all investigations are carried out within the framework of scattering theory. The thesis comprises four papers.

In Paper I we propose a thermoelectric heat engine in a two terminal quantum Hall conductor, based only on quantum interference and with efficiency and power production close to the theoretical maximum.

In Paper II we theoretically compare the combined energy and charge transport properties of different single electron sources in mesoscopic systems.

In Paper III we analyze a quantum point contact as a thermoelectric heat engine, exploring the trade-off between efficient operation, large power output and small fluctuations.

In Paper IV we investigate the interplay between thermoelectric transport properties and single electron sources, focusing on the role of quantum screening effects.

Key words
Thermoelectricity, Single electron source, Scattering theory, Mesoscopic physics

Classification system and/or index terms (if any)

Supplementary bibliographical information

Language
English

ISSN and key title

ISBN
978-91-7895-326-4 (print)
978-91-7895-327-1 (pdf)

Recipient's notes

Number of pages
65

Price

Security classification

Signature _____ Date 2019-10-07

Thermoelectric Effects and Single Electron Sources in Mesoscopic Transport; a Scattering Approach

by Sara Kheradsoud

LUND
UNIVERSITY

A doctoral thesis at a university in Sweden takes either the form of a single, cohesive research study (monograph) or a summary of research papers (compilation thesis), which the doctoral student has written alone or together with one or several other author(s).

In the latter case the thesis consists of two parts. An introductory text puts the research work into context and summarizes the main points of the papers. Then, the research publications themselves are reproduced, together with a description of the individual contributions of the authors. The research papers may either have been already published or are manuscripts at various stages (in press, submitted, or in draft).

Cover illustration front: A 2-D plot of the thermoelectric power maximized over potential bias respect to the applied temperature difference and energy steps of a quantum point contact. (Adapted from Paper III).

Funding information: Supported by the People Program (Marie Curie Actions) of the European Union's Seventh Framework Program (FP7-People-2013-ITN) under REA grant agreement n°608153, PhD4Energy.

Faculty of Science, Department of Physics

ISBN: 978-91-7895-326-4 (print)
ISBN: 978-91-7895-327-1 (pdf)

Printed in Sweden by Media-Tryck, Lund University, Lund 2019

Contents

List of publications and contributions of the author

This thesis is based on the following publications, referred to by their Roman numerals:

I **Optimal Quantum Inteference Thermoelectric Heat Engine with Edge States**

Peter Samuelsson, Sara Kheradsoud, Björn Sothmann
Phys. Rev. Lett. **118**, 256801 (2017)

We consider a mesoscopic system where the thermoelectric performance is solely due to quantum interference. The system is a two-terminal electronic Mach-Zehnder interferometer with a mesoscopic capacitor coupled to one of the interfereometer arms. We demonstrate that the maximum power and corresponding efficiency can reach 90 % and 83 %, respectively, of the theoretical maximum. The proposed heat engine can be realized with existing experimental techniques and has a performance robust against moderate dephasing.

Contribution: Based on the calculation I did for a preliminary project, the idea of this work was developed. I performed some of the calculations and participated in discussions of the formulation of the manuscript.

II **Minimal excitation single-particle emitters: Comparison of charge-transport and energy-transport properties**

Nastaran Dashti, Maciej Misiorny, Sara Kheradsoud, Peter Samuelsson, Janine Splettstoesser
Phys. Rev. B. **100**, 035405 (2019)

We investigate different types of time-dependently driven single-particle sources whose common feature is that they produce pulses of integer charge and minimally excite the Fermi sea. We explore how the basic differences of the sources impact time- and energy-resolved charge and energy currents, as well as their zero-frequency correlators. In particular, we are able to characterize and quantify the effect of temperature on the transport properties by a small set of physically relevant parameter ratios.

Contribution: I did some of the calculations, both analytical and numerical. I also produced initial plots, comparing analytical and numerical approaches. For the writing of the manuscript, I participated in the discussions concerning overall structure and detailed formulations.

III **Power, Efficiency and Fluctuations in a Quantum Point Contact as Steady-State Thermoelectric Heat Engine**

Sara Kheradsoud, Nastaran Dashti, Maciej Misiorny, Patrick P. Potts, Janine Splettstoesser, Peter Samuelsson
Entropy **2019**, 21(8), 777

We present an analysis of the trade-off between large power output, high efficiency and small fluctuations in the operation of a heat engine realized in a quantum point contact. In particular, we investigate the bound jointly imposed on the power, efficiency, and fluctuations by a recently derived thermodynamic uncertainty relation. It is found that for a broad range of parameters, the power production reaches nearly its theoretical maximum value, with efficiencies more than half of the Carnot efficiency and at the same time with rather small fluctuations.

Contribution: I did most of the numerical calculations and obtained the data for all plots. I also performed some of the analytical calculations. Moreover, I prepared parts of the first draft of the manuscript and contributed to the discussion of the results.

IV **Screening effects in the interplay between thermoelectrics response and time-dependent driving**

Nastaran Dashti, Sara Kheradsoud, Maciej Misiorny, Peter Samuelsson, Janine Splettstoesser
(Manuscript in preparation)

We investigate the interplay between thermoelectric effects and the transport properties of a single electron source, accounting for screening effects in the weakly nonlinear transport regime. The thermoelectric effects arise due to energy dependent scattering at a quantum point contact. As a main result we find that the linear-response transport coefficients modified by the source operation give direct access to rather unexplored quantum screening effects, which in other types of devices are obscured by geometric capacitive effects.

Contribution: I performed some of the calculations, both analytical and numerical. I contributed to the discussion of the results and the formulation of the manuscript.

Acknowledgements

I would like to acknowledge all people who made this thesis to happen by their help and support. I just want to emphasize that I am grateful to all people I met during these years even though I do not mention their names here.

First of all I would like to thank my supervisor Peter Samuelsson. Thank you for giving me the opportunity to work in your group and appreciate all your continued support whenever I needed . Thank you to be patient with me and your door was always open to me to discuss any matter regardless of its minor or major importance.

I also want to thank all former and current people in our research group during my PhD time at Lund University. It was a great pleasure to work with Tineke van den Berg, Ognjen Malkoc, Fredrik Brange, Patrick Potts, Bahareh Goldozian, Timo Kerremans (also officemate) and Björn Annby Andersson.

I would also like to thank the scientists from outside our Division who I collaborated with: Björn Sothmann from University of Duisburg-Essen, and Janine Splettstoesser, Nastaran Dashti, Maciek Misiorny at Chalmers university. Thank you for your hospitality each time I came to Gothenburg and all Wednesdays Skype meetings.

I want to thank people from "Quantum Wise" company; Kurt Stokbro, Line Jelver, Umberto Martinez and specially Daniele Stradi for the collaboration and help while I was doing my secondment in Copenhagen.

My officemates over these years, Miroslav Hopjan, Jakob Bengtsson, Stefano, Ran Si, Ekin Önder, and Rashi Sachdeva were a source of joy for me. Thank you all. With your presence, you made our office a friendly and nice place to work. I enjoyed your company and all interesting discussion about physics, sports, cultures, philosophy, politics, and beyond. I learned a lot from you and I am grateful for that.

I also want to thank Fikeraddis Damtie, Asimina Papoulia, Gunnar Eriksson, Zhen Zhao, Alex Arash Sand Kalaee, Martin Albertsson, Mattias Bertolino, Josef Josefi, Megha Gopalakrishna, Andrea Idini, David Winge, Daniel Ward, Jon Grumer, Fredrik Nilsson and all other people at the Division of Mathematical physics. I enjoyed all fun and good time with all of you on many occasions. Thank you for organizing and participating in social events of our division and creating a wonderful "memorybank" for me from my time in Lund. Thank you Claudio Verdozzi for giving good advices regarding thesis and life. I am really grateful to Katarina Lindqvist and Cecilia Jarlskog. Thank you Katarina for all your generous help with administrative matters and everything. Dear Cecilia your presence in our division is valuable. Thank you for all your help with my thesis.

I thank all my friends in my hometown, specially Shima. You made my vacations back

home wonderful, fun and memorable and always surprised me with organizing warm and friendly parties and great hiking trips. I also want to thank my dear friends outside Lund. Thank you Sara for all your supports and love. You shared your helpful experiences with me whenever I was about to give up. I am also thankful to Azar. You have been always ready to help me with small and big things.

Last but foremost, I want to express my gratitude to my family specially my parents who brought me to this world and did their best to support and encourage me on my way in life. Without their sincere love and help I would not be where I am now.

Popular summary in English

As we all know access to energy is an ever-increasing prerequisite for functioning of modern societies. There are several essential aspects of this matter which are often discussed such as old and new sources of energy, their sustainability as well as possible contribution to pollution. An issue which has become more and more important is how to recover the energy which is often wasted and dissipated and re-use it for useful applications.

One type of energy which we see being wasted everywhere in our daily life is heat. According to the second law of thermodynamic, nature does not allow us to convert 100 percent of the heat energy to useful work. Nonetheless, we have realized that heat should be looked upon as a new source of energy and useful work. Thermoelectric science and technology studies, both theoretically and experimentally, have paved the way to harnessing this seemingly wasted energy and thus contribute to the resources issue as well as protecting nature by providing a clean energy source.

For converting heat to energy, electricity is produced between two reservoirs with different temperatures. This procedure makes use of developments in nanoscience and nanotechnology where it was realized that in small scale systems which are confined in one or two directions we see stronger effects of thermoelectricity. This is due to being able to filter out the electrons based on their energies whereby only electrons with preselected amount of energy are able to create electrical current.

In experiments, related to the work presented in this thesis, a major domain of research has been devoted to developing and fabricating different materials in order to improve the thermoelectric properties of the set ups in order to obtain reasonable amount of work for specific temperature differences. However, from the theoretical point of view, the main driving force has been to learn about new physical features of nano-scale and mesoscopic scale systems and employ them for exactly the same reason as experimentalists do.

Another topic which also has been studied in mesoscopic systems is single-electron emission, a phenomenon which is important for development of modern electronic devices. In general electrons can be emitted from the surface of a material if it is subject to various external stimuli, such as heat, photons, ions, or other electrons, and large electric fields. In this thesis we have used the latter source to stimulate the controlled emission of electrons within a mesoscopic conductor, giving rise to an electrical current.

An anticipated application domain for single-electron source is quantum information technology, where in order to transfer the information accurately it is important to have full control over the number of electrons which are supposed to responsible for this transport.

As we know physics is the science of what can be said about nature and tested by measurements. As long as a hypothesis has not been checked experimentally it is no more than a

speculation. This collaboration theory-experiment has been very fruitful in promotion and understanding of our science. For example, in order to measure a physical quantity we have to first define a universal unit for it which is accurate and accessible all around the world at any time. It is rewarding to see that the single-electron sources were recently exploited to define a universal unit for Ampere, the unit of electrical current.

Part I

Background and Theory

Chapter 1

Introduction

The title of this thesis is Thermoelectric effects and single electron sources in mesoscopic transport; a scattering approach. To provide an introduction to the thesis, it is natural to describe the different terms of the title and explain why they brought together constitute an interesting and timely topic for a doctoral thesis. However, the order or appearance of the terms in the title does not provide the most clear and logical order for a presentation, instead we first discuss mesoscopic transport, thereafter thermoelectric effects and single electron sources and, as the last term, the scattering approach.

Mesoscopic describes something which is between macroscopic, or large, the world governed by the laws of classical, Newtonian mechanics, and microscopic, or small, goverened by the laws of quantum mechanics. The field of mesoscopic physics [1], at the interface between macro- and microscopic, combines concepts and ideas from both the large and the small, classical statistical mechanics with quantum coherent phenomena, classical models of transport with the wave-like nature of electrons. Mesoscopic physics emerged as a research field in the 1980s, when experiments on sub-micrometer electronic structures at cryogenic temperatures reached such a quality and level of control that the quantum nature of charge carriers started to become relevant [2]. A number of novel, mesoscopic phenomena were discovered and explored, such as weak localization [3], conductance quantization [4, 5] and universal conductance fluctuations [6, 7]. Following the early development, focusing on electronic transport in semiconductor and normal metallic conductors, the field has expanded to cover for example superconducting, ferromagnetic and topological systems.

One area of mesosocpic physics which has received increasing attention over the last decades is thermoelectric transport. The key idea of the broad field of thermoelectricity is to convert heat to electrical work. One strong motivation is to develop novel technologies for recovering waste heat and provide solutions to the worlds energy challenges. In

mesoscopic thermoelectrics [8, 9], the scope is typically more modest, with a focus on fundamental physical effects in charge and energy transport. The aim with many investigations is to propose, analyse and demonstrate novel mechanisms for energy harvesting, conversion and transport, often via proof-of-concept models and experiments. Although this type of basic science constitutes the first steps in the development of novel technology, to take the novel concepts from cryogenic temperatures in a controlled laboratory environment to useful devises in our everyday life is typically a daunting task.

Another recent area of mesoscopic physics which has a lot of potential for applications is single or few-particle sources of charge carriers, that is, ways to time-control the emission of individual electrons or holes, from a localized source out into a conductor, resulting in an electrical current [10, 11]. One important example of applications of such sources is metrology, the science of measuring, where the new definition of the Ampere in terms of the elementary charge makes sources that can emit a given number of electrons in a well defined time highly useful. Of more interest to fundamental transport experiments are the types of on-demand sources that produce a noiseless stream of single electron or hole excitations, at energies close to the Fermi energy [12, 13]. These sources have been used to perform electron quantum optics experiments, that is, experiments where electrons propagate, scatter and collide in ballistic structures, electronic analogs of single photon, quantum optics experiments.

A common denominator for these areas of mesoscopic physics is that the basic physical phenomena can be described by a scattering approach to transport [14]. Underpinning the idea of describing electronic transport in terms of scattering is the insight of Landauer that "conductance is transmission" [15]. Building on this idea, the modern theory of scattering for quantum transport was developed during the early days of mesoscopic physics. Often referred to as the Landauer-Büttiker approach [16], it has due to the combination of conceptual simplicity and wide applicability become one of the basic tools for describing quantum transport in general. While originally developed to describe average currents, it has also successfully been employed to explain noise and fluctuations in transport [17].

The work in this thesis concerns both thermoelectric phenomena and physics of single electron sources, in mesoscopic systems. The main aim for the work has been to theoretically explore novel phenomena within these areas, both separately and by combining them. As is typically the case for mesoscopic theory, a strong motivation has been to propose, model and analyse experiments that could test or demonstrate the predicted phenomena. To put the work in a proper context and to provide the necessary background, the rest of the thesis has been organized as follows. In Chapter 2 we introduce scattering theory for time-independent systems, discussing both average current and current correlations. In Chapter 3, the scattering theory is extended to describe also time-dependent, periodically driven systems. This Floquet scattering theory is of key importance to describe on-demand electron sources. Chapter 4 is devoted to thermoelectricity. A scattering theory for both

charge and energy is presented and basic properties of thermoelectric heat engines are discussed. In Chapter 5 we discuss on-demand electron sources, focusing on the time-driven mesoscopic capacitor[12, 18]. Finally, in Chapter 6 we provide a brief description of the content of the papers I to IV.

Chapter 2

Time-independent scattering theory

The modern theory of scattering, often referred to as the Landauer-Büttiker scattering approach, provides a physically intuitive framework for describing quantum transport in mesoscopic and nanoscale conductors. Scattering theory has over the last decades been employed to describe a wide variety of transport phenomena, such as the flow of charge, energy and spin, both average currents as well as noise and fluctuations[17]. Conductors ranging from diffusive metals [19] to ballistic semiconductors [2], coupled to superconducting or ferromagnetic terminals [20], have successfully been characterized by scattering approaches. Originally developed to describe time-independent steady-state transport in phase coherent conductors in the linear response regime, scattering approaches have also been employed to account for phase-breaking processes [21–24], non-linear effects [25, 26] and time-periodically driven systems [27]. In this chapter we review the basics of time-independent scattering theory. We first present a more qualitative, single particle approach and discuss some key transport concepts. Thereafter we provide a more thorough derivation, fully accounting for the fermionic nature of the electrons by employing the second quantization formalism. This formalism properly captures the anti-symmetrization of the many-particle wavefunction and allows for a calculation of fluctuations, or noise, of transport properties. The time-independent scattering approach is used to derive the results in papers I and III, also of importance for the calculations in papers II and IV.

2.1 Single particle description

To describe the basic concepts of time-independent scattering theory, we consider a generic, multi-terminal mesoscopic conductor, see Fig.2.1. The conductor consists of a phase coherent scattering region connected to N terminals via perfectly ballistic leads. All in-

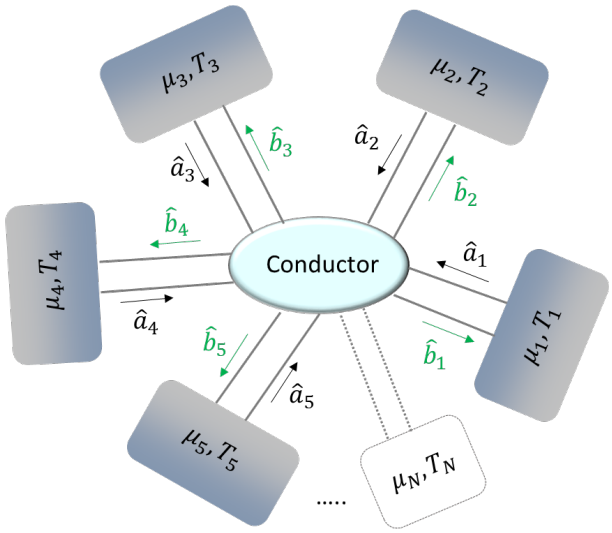

Figure 2.1: Schematic of a multi-terminal system consisting of a mesoscopic scatterer coupled via ballistic leads to N electronic reservoirs, kept at temperatures T_α and chemical potentials μ_α ($\alpha = 1, 2, 3, \ldots, N$). Annihilation operators $\hat{a}_\alpha$ refer to particles which are incident from the reservoir α towards the scatterer. Similarly $\hat{b}_\alpha$'s refer to the particles which are propagating away from the scatterer, towards reservoir α. The direction of propagation of the particles is denoted with arrows.

formation about the scattering region is comprised in a scattering matrix S. Formally, the scattering matrix is obtained from the solution of the Schrödinger equation in the scattering region, which for most conductors is a non-trivial task. Here we will however keep maximum generality and present the discussion [17] and the results directly in terms of the elements of S. The N terminals are electronic reservoirs at thermal equilibrium. Each terminal $\alpha = 1, \ldots, N$ is kept at an electro-chemical potential $\mu_\alpha = eV_\alpha + \mu_0$, with V_α the electrical potential, and a temperature T_α. In the general case, each lead can support M_α conduction modes. The wave function $\psi_\alpha(E, \mathbf{r}_\alpha)$ for an electron of effective mass m, at energy E in lead α, is given by the general solution to the time-independent Schrödinger equation. Far away from the scatterer, it can be written as

$$\psi_\alpha(E, \mathbf{r}_\alpha) = \sum_{j=1}^{M_\alpha} \frac{\phi_{\alpha_j}(y_\alpha, z_\alpha)}{\sqrt{hv_{\alpha_j}}} \left[a_{\alpha_j}(E) e^{ik_{\alpha_j}(E)x_\alpha} + b_{\alpha_j}(E) e^{-ik_{\alpha_j}(E)x_\alpha} \right], \qquad (2.1)$$

where $\mathbf{r}_\alpha = [x_\alpha, y_\alpha, z_\alpha]$ (using a local coordinate system) and $\phi_{\alpha_j}(y_\alpha, z_\alpha)$ is the transverse component of the wavefunction of mode j in lead α, with eigenenergy E_{α_j}. The corresponding wave number is $k_{\alpha_j}(E) = \sqrt{2m(E - E_{\alpha_j} - \mu_0)/\hbar^2}$ and the velocity $v_{\alpha_j}(E) = \hbar k_{\alpha_j}(E)/m$. Inside the ballistic leads the electrons can move freely along the longitudinal direction x_α. The coefficients a_{α_j} and b_{α_j} are the current amplitudes for waves propagating towards and away from the scatterer, respectively.

To calculate the electrical current carried by an electron described by the wavefunction $\psi_\alpha(E, \mathbf{r}_\alpha)$, we insert the expression in Eq. 2.1 into the quantum mechanical expression for the current density. By further integrating the current density over the transverse coordinates and over all energies we obtain the total current flowing through a cross-section of lead α, given by

$$I_\alpha = \frac{e}{h} \int dE \sum_{j=1}^{M_\alpha} \left(|a_{\alpha_j}(E)|^2 - |b_{\alpha_j}(E)|^2 \right). \tag{2.2}$$

The current amplitudes b_{α_j}, for particles propagating away from the conductor in lead α and mode α_j, are related to the amplitudes a_{β_i}, for a particle incident on the scatterer in lead β and mode β_i, via the elements of the scattering matrix S of the conductor as

$$b_{\alpha_j} = \sum_{\beta=1}^{N} \sum_{i=1}^{M_\beta} S_{\alpha_j,\beta_i} a_{\beta_i}. \tag{2.3}$$

The modulus squared of an element of the scattering matrix, $|S_{\alpha_j,\beta_i}|^2$, yields the probability for a particle to scatter from mode i in lead β to mode j in lead α. The scattering matrix can conveniently be written on a matrix block form as

$$S = \begin{pmatrix} \mathbf{S}_{11} & \mathbf{S}_{12} & \cdots \\ \mathbf{S}_{21} & \mathbf{S}_{22} & \cdots \\ \vdots & \vdots & \ddots \end{pmatrix}. \tag{2.4}$$

Here each matrix block $\mathbf{S}_{\alpha\beta}$[1] contains all amplitudes to scatter from lead β to lead α. One can thus write the block as

$$\mathbf{S}_{\alpha\beta} = \begin{pmatrix} S_{\alpha_1,\beta_1} & S_{\alpha_1,\beta_2} & \cdots \\ S_{\alpha_2,\beta_1} & S_{\alpha_2,\beta_2} & \cdots \\ \vdots & \vdots & \ddots \end{pmatrix}. \tag{2.5}$$

We point out that the dimension of the scattering matrix is determined by the number of modes and terminals. For example, for a system with two terminals and three transport modes in each lead, S will be a 6×6 matrix. If we instead have a system with four terminals coupled to the conductor via single mode leads S will be of dimension 4×4. In general the dimension of the scattering matrix is $M_T \times M_T$, where $M_T = \sum_\alpha M_\alpha$, the total number of modes in all the leads.

Due to the requirement of current conservation for scattering at the conductor, the scattering matrix is unitary, that is

$$SS^\dagger = S^\dagger S = 1. \tag{2.6}$$

[1]Throughout this thesis we use boldface to denote the scattering matrix block in mode space.

Here the dagger † denotes a Hermitian conjugation, or a transpose of the matrix and a complex conjugation of all elements. In terms of matrix blocks the unitarity implies that

$$\sum_{\beta=1}^{N} \mathrm{tr}\left[\mathbf{S}^{\dagger}_{\alpha\beta}\mathbf{S}_{\gamma\beta}\right] = \delta_{\alpha\gamma}, \tag{2.7}$$

for any α, γ. Note that throughout this chapter we denote $\mathbf{S}^{\dagger}_{\alpha\beta} = [\mathbf{S}_{\alpha\beta}]^{\dagger}$.

To calculate the current flowing in the leads of the conductor as a result of an applied electrical and/or thermal bias at the terminals, we need to specify the boundary conditions for the incoming amplitudes. Since the terminals are at thermal equilibrium, the occupation probability at energy E in terminal α is given by the Fermi-Dirac distribution,

$$f_{\alpha}(E) = \frac{1}{1 + e^{(E-\mu_{\alpha})/(k_B T_{\alpha})}}. \tag{2.8}$$

It can be shown that the occupation probability for particles emitted from terminal α, incident on the conductor in any mode α_j at energy E, is given by the Fermi-Dirac distribution of the corresponding terminal. That is, we have $|a_{\alpha_j}(E)|^2 = f_{\alpha}(E)$ for all j.

Starting from the current expression in Eq. (2.2), writing the outgoing amplitudes b_{α_j} in terms of the incoming ones, a_{β_i}, and using that the terminal boundary conditions can be written $a_{\alpha_j}(E)a^{*}_{\beta_i}(E) = f_{\alpha}(E)\delta_{\alpha\beta}\delta_{ij}$ (to be motivated rigorously below) we arrive at

$$I_{\alpha} = \frac{e}{h}\int dE \sum_{\beta=1}^{N} \mathrm{tr}\left[\mathbf{S}^{\dagger}_{\alpha\beta}\mathbf{S}_{\alpha\beta}\right][f_{\alpha}(E) - f_{\beta}(E)], \tag{2.9}$$

where the trace "tr" is taken over the modes and we have used the unitarity relation in Eq. (2.7).

In particular, for a two terminal system, shown in Fig. 2.1, we can write the current flowing from terminal left L to right R as

$$I = \frac{e}{h}\int dE\, \mathrm{tr}\left[\mathbf{S}^{\dagger}_{LR}\mathbf{S}_{LR}\right][f_{L}(E) - f_{R}(E)]. \tag{2.10}$$

Furthermore, considering the case where the scattering matrix elements are independent on energy on the scale of the applied voltage V and background temperature, we have

$$I = \frac{e^2}{h} V\, \mathrm{tr}\left[\mathbf{S}^{\dagger}_{LR}\mathbf{S}_{LR}\right]. \tag{2.11}$$

Hence, the electrical conductance $G = dI/dV$ is given by

$$G = G_0\, \mathrm{tr}\left[\mathbf{S}^{\dagger}_{LR}\mathbf{S}_{LR}\right], \quad G_0 = \frac{e^2}{h}, \tag{2.12}$$

which is just the Landauer formula [1] for the conductance of a multi-mode conductor. The quantity G_0 is the (single spin) conductance quantum. For a single mode conductor, introducing the transmission probability $D = |S_{LR}|^2$, we have $G = G_0 D$, explicitly demonstrating that conductance in mesoscopic conductors is all about transmission.

2.2 Second quantization description

Electrons are fermions, having a many-particle wave-function which is anti-symmetrized, that is, it changes sign under the exchange of any two particles. As a consequence, electrons obey the Pauli exclusion principle, prohibiting two identical particles to be at the same spatial location. This has consequences for physical quantities that depend on the correlation between electrons, such as the fluctuations, or noise, of transport properties. In order to account for the fermionic nature of electrons, it is convenient to work in the second quantization formalism. Below we provide a careful derivation of the key quantities needed for a scattering theory of transport, formulated within second quantization. To simplify the notation we in this section, and in the major part of the thesis, consider leads that only support one conducting mode.

As a starting point we define $\hat{a}^\dagger_\alpha(E)$ ($\hat{a}_\alpha(E)$) as an operator which creates (annihilates) electrons with energy E in the lead α, propagating towards the scatterer, see Fig. 2.2. In the same way, the creation $\hat{b}^\dagger_\alpha(E)$ and annihilation $\hat{b}_\alpha(E)$ operators describe electrons which get scattered from the conductor, propagating out towards terminal α. The annihilation operators $\hat{a}_\alpha$ and $\hat{b}_\beta$ are related by the scattering matrix elements $S_{\beta\alpha}$ as

$$\hat{b}_\beta(E) = \sum_\alpha S_{\beta\alpha}(E)\hat{a}_\alpha(E). \tag{2.13}$$

The fermionic nature of the electrons are accounted for by the anti-commutation relations for the operators, as

$$\begin{aligned} \{\hat{a}^\dagger_\alpha(E), \hat{a}_\beta(E')\} &= \delta_{\alpha\beta}\delta(E-E'), \\ \{\hat{a}^\dagger_\alpha(E), \hat{a}^\dagger_\beta(E')\} &= 0, \\ \{\hat{a}_\alpha(E), \hat{a}_\beta(E')\} &= 0, \end{aligned} \tag{2.14}$$

and equivalently for $\hat{b}^\dagger_\alpha(E), \hat{b}_\beta(E')$.

We can then define the electron creation field operator in a lead α as

$$\hat{\Psi}_\alpha(\mathbf{r}_\alpha, t) = \int \frac{dE}{\sqrt{h v_\alpha(E)}} e^{-iEt/\hbar}\phi_\alpha(y_\alpha, z_\alpha)[\hat{a}_\alpha(E)e^{ik_\alpha(E)x_\alpha} + \hat{b}_\alpha(E)e^{-ik_\alpha(E)x_\alpha}]. \tag{2.15}$$

Here the transverse wavefunction $\phi_\alpha(y_\alpha, z_\alpha)$, the wavenumber $k_\alpha(E)$ and the velocity $v_\alpha(E)$ are defined in connection to the wave function in Eq.(2.1).

The current density operator $\hat{\mathbf{j}}_\alpha(\mathbf{r}_\alpha, t)$ in lead α can be defined in terms of field operators as

$$\hat{\mathbf{j}}_\alpha(\mathbf{r}_\alpha, t) = \frac{\hbar e}{2mi}\left[\hat{\Psi}_\alpha^\dagger \nabla\hat{\Psi}_\alpha - (\nabla\hat{\Psi}_\alpha^\dagger)\hat{\Psi}_\alpha\right]. \tag{2.16}$$

Then the operator for the current flowing along the x_α direction in lead α will be defined as an integral of the current density over the cross section of the lead, as

$$\hat{I}_\alpha(x_\alpha, t) = \int_{S_\alpha} \hat{\mathbf{j}}(\mathbf{r}, t)\cdot\hat{\mathbf{n}}dS, \tag{2.17}$$

where $\hat{\mathbf{n}}_\alpha$ is the cross section normal vector and S_α is its area.

To obtain an expression for the current operator we note that the velocity $v_\alpha(E)$ does not change significantly on the typical energy scales of the system (applied bias, temperature etc), and is much smaller than the Fermi energy. That is, all net transport in mesoscopic systems occurs close to Fermi energy. We can then substitute $v(E) \approx v(\mu_0)$ in the denominator in Eq.(2.15). As a consequence the current operator integral in Eq.(2.17) can be evaluated, giving

$$\hat{I}_\alpha(t) = \frac{e}{h}\int\int dEdE' e^{i\frac{E-E'}{\hbar}t}\left\{\hat{b}_\alpha^\dagger(E)\hat{b}_\alpha(E') - \hat{a}_\alpha^\dagger(E)\hat{a}_\alpha(E')\right\}. \tag{2.18}$$

This expression for the current operator serves as a starting point for the discussion of both average current and noise, in the following.

2.2.1 Average current

The average, measured current is obtained by taking a quantum-statistical average, denoted $\langle..\rangle$, of the current operator as $I_\alpha = \langle\hat{I}_\alpha\rangle$. The average of the product of second quantization operators for particles emitted from a reservoir α is, as discussed above, determined by the properties of the reservoir and not affected by the scattering at the mesoscopic conductor. It can be written

$$\langle\hat{a}_\alpha^\dagger(E)\hat{a}_\beta(E')\rangle = \delta_{\alpha\beta}\delta(E-E')f_\alpha(E), \tag{2.19}$$

where the Fermi-Dirac distribution $f_\alpha(E)$ is given in Eq.(2.8). However, for the particles scattered back from the conductor, the same equilibrium condition does not hold. Therefore, to calculate the average over the product of operators $\hat{b}^\dagger(E)\hat{b}^\dagger(E')$, we first need to write them in terms of the operators $\hat{a}$ and $\hat{a}^\dagger$, making use of the scattering matrix relation in Eq.(2.13). With this the average current flowing in the lead α, due to the electrical

potential (or thermal) bias applied at the terminals can be written as,

$$I_\alpha = \frac{e}{h}\int dE \left\{ f_\alpha^{(out)}(E) - f_\alpha(E) \right\}, \tag{2.20}$$

where the distribution function for the scattered electrons, going out from the conductor, is given by

$$f_\alpha^{(out)}(E) = \sum_\beta |S_{\alpha\beta}(E)|^2 f_\beta(E). \tag{2.21}$$

One can thus understand the expression for $f_\alpha^{(out)}(E)$ as follows: electrons distributed according to $f_\beta(E)$ are emitted from terminal β and scattered with probability $|S_{\alpha\beta}(E)|^2$ to lead α, moving away from the scatterer towards terminal α.

Putting this together and making use of the unitarity condition $\sum_\beta |S_{\alpha\beta}|^2 = 1$ we can write the average current in lead α as

$$I_\alpha = \frac{e}{h}\int dE \sum_\beta |S_{\alpha\beta}(E)|^2 (f_\beta(E) - f_\alpha(E)). \tag{2.22}$$

This expression for the average current will be used throughout the thesis. We stress that in all discussion we consider the single-spin case, accounting for spin will only multiply all derived quantities by a factor of two.

In the linear response regime in applied bias voltage, assuming the temperature of all terminals to be the same, $T_\alpha = T$, we can expand all Fermi distribution functions in Eq. (2.8) as

$$f_\alpha(E) = f(E) - eV_\alpha \frac{df(E)}{dE}, \quad f(E) = \frac{1}{1 + e^{(E-\mu_0)/(k_B T)}}, \tag{2.23}$$

where $f(E)$ is the equilibrium distribution function. We can then write the average current

$$I_\alpha = \frac{e^2}{h}\left[V_\alpha - \sum_\beta V_\beta \int dE \frac{df(E)}{dE} |S_{\alpha\beta}(E)|^2 \right]. \tag{2.24}$$

The conductance then becomes

$$G_{\alpha\beta} = \frac{dI_\alpha}{dV_\beta} = \frac{e^2}{h}\left[\delta_{\alpha\beta} - \int dE \frac{df(E)}{dE} |S_{\alpha\beta}(E)|^2 \right]. \tag{2.25}$$

In the case with a two-terminal system, considering $G = G_{12} = G_{21}$, we recover the Landauer result in Eq.(2.12), for single channel leads.

2.2.2 Current noise

As pointed out above, the second quantization approach allows us to investigate electrical current fluctuations, or noise, within the same framework. We first start with a formal derivation of the noise expressions, largely following Büttiker [28–30]. Based on the derived expressions we provide qualitative explanations for the different terms contributing to the noise.

The starting point for the calculation is the expression for the (symmetrized) correlator of current fluctuations at terminals α and β,

$$P_{\alpha\beta}(t-t') \equiv \frac{1}{2}\langle \Delta\hat{I}_\alpha(t)\Delta\hat{I}_\beta(t') + \Delta\hat{I}_\beta(t')\Delta\hat{I}_\alpha(t)\rangle, \tag{2.26}$$

where we define the fluctuation operator

$$\Delta\hat{I}_\alpha(t) = \hat{I}_\alpha(t) - \langle\hat{I}_\alpha\rangle, \tag{2.27}$$

and note that in the steady state, without time-dependent system parameters, the correlator $P_{\alpha\beta}$ only depends on time differences. The frequency dependent correlator is obtained by a Fourier transformation as

$$P_{\alpha\beta}(\omega) = \int_{-\infty}^{\infty} dt\, e^{i\omega t} P_{\alpha\beta}(t). \tag{2.28}$$

In this thesis we are only interested in the zero frequency correlator and will thus consider

$$P_{\alpha\beta} \equiv P_{\alpha\beta}(0) = \int_{-\infty}^{\infty} dt P_{\alpha\beta}(t). \tag{2.29}$$

Noting that the current fluctuation correlator can be written

$$\langle\Delta\hat{I}_\alpha(t)\Delta\hat{I}_\beta(t')\rangle = \langle\hat{I}_\alpha(t)\hat{I}_\beta(t')\rangle - \langle\hat{I}_\alpha(t)\rangle\langle\hat{I}_\beta(t')\rangle. \tag{2.30}$$

We can then insert the expression for the current operator in Eq.(2.18) into the equation for the zero frequency correlator, Eq.(2.29). Following the same procedure as for the average current, we express the $\hat{b}$-operators in terms of the $\hat{a}$-operators and the scattering matrix elements. However, in addition to the average current calculations, for the term $\langle\hat{I}_\alpha(t)\hat{I}_\beta(t')\rangle$ we now need to evaluate the quantum statistical average of four $\hat{a}$-operators giving (using Wick's theorem) [31]

$$\begin{aligned}
&\langle\hat{a}^\dagger_\alpha(E)\hat{a}_\beta(E')\hat{a}^\dagger_\gamma(E'')\hat{a}_\delta(E''')\rangle = \langle\hat{a}^\dagger_\alpha(E)\hat{a}_\beta(E')\rangle\langle\hat{a}^\dagger_\gamma(E'')\hat{a}_\delta(E''')\rangle \\
+ \;& \langle\hat{a}^\dagger_\alpha(E)\hat{a}_\delta(E''')\rangle\langle\hat{a}_\beta(E')\hat{a}^\dagger_\gamma(E'')\rangle \\
= \;& \delta_{\alpha\beta}\delta_{\gamma\delta}\delta(E-E')\delta(E''-E''')f_\alpha(E)f_\gamma(E'') \\
+ \;& \delta_{\alpha\delta}\delta_{\beta\gamma}\delta(E-E''')\delta(E'-E'')f_\alpha(E)[1-f_\gamma(E'')].
\end{aligned} \tag{2.31}$$

Here in the middle step we have written out explicitly the two different possible pairings of the creation and annihilation operators. The first, direct pairing term, will directly cancel the contribution coming from $\langle \hat{I}_\alpha(t)\rangle\langle \hat{I}_\beta(t')\rangle$ in the total correlator expression. The second, exchange term, is thus what gives rise to the noise.

Making use of the expression in Eq.(2.31) in the evaluation of the noise, we arrive after some calculations at

$$\begin{aligned} P_{\alpha\beta} &= \frac{e^2}{h}\sum_{\gamma\delta}\int dE(\delta_{\alpha\gamma}\delta_{\alpha\delta} - S^*_{\alpha\gamma}S_{\alpha\delta})(\delta_{\beta\gamma}\delta_{\beta\delta} - S^*_{\beta\delta}S_{\beta\gamma}) \\ &\times \{f_\gamma(E)[1-f_\delta(E)] + f_\delta(E)[1-f_\gamma(E)]\}, \end{aligned} \tag{2.32}$$

where we note that the energy dependence of the scattering matrix elements is not explicitly written out. This expression is naturally understood as consisting of two qualitatively different parts. First, by considering the equilibrium situation, where all distribution functions are given by $f_\alpha(E) = f(E)$, with $f(E)$ the equilibrium distribution function, we get the noise

$$P_{\alpha\beta} = -\frac{2e^2k_BT}{h}\int dE\frac{df}{dE}(2\delta_{\alpha\beta} - |S_{\alpha\beta}|^2 - |S_{\beta\alpha}|^2), \tag{2.33}$$

where we made use of the relation $f(E)[1-f(E)] = -df(E)/dE$ and the unitary relation in Eq.(2.7). By comparing to Eq.(2.25) we see that we can write

$$P_{\alpha\beta} = 2k_BT(G_{\alpha\beta} + G_{\beta\alpha}). \tag{2.34}$$

That is, the equilibrium noise can be written in terms of conductances of the system only, something which also can be understood in terms of the fundamental fluctuation-dissipation theorem [17, 32]. As a consequence, the equilibrium noise, also called thermal noise, does not provide any more information about the system beyond the average current. In fact, the origin of the noise is the fluctuations of the occupation numbers in the reservoirs due to finite temperature.

Second, by considering the case of zero temperature, $T = 0$, the Fermi functions are reduced to step-functions in energy and we can write

$$\begin{aligned} P_{\alpha\beta} &= \frac{e^2}{h}\sum_{\gamma\neq\delta}\int dE\, S^*_{\alpha\gamma}S_{\alpha\delta}S^*_{\beta\delta}S_{\beta\gamma} \\ &\times \{f_\gamma(E)[1-f_\delta(E)] + f_\delta(E)[1-f_\gamma(E)]\}. \end{aligned} \tag{2.35}$$

This is the non-equilibrium, or shot-noise part. As is clear from the expression, this part of the noise can not be written in terms of the average currents and thus contains information about the scatterer beyond what can be inferred from current measurements only. The origin of this noise term is the probabilistic, quantum nature of the scattering processes.

We also note that correlations between currents in the same terminal, that is for $\alpha = \beta$, the noise $P_{\alpha\alpha}$ in Eq.(2.32) is called the auto-correlator, while correlations between currents in different terminals, $\alpha \neq \beta$, the noise $P_{\alpha\beta}$ is called the cross-correlator.

2.3 Two-terminal conductor; current, noise and Fano factor

Of special importance is the case with a two-terminal conductor, shown in Fig. 2.2, labelling the two terminals L and R. The transmission probability is denoted, for brevity by, $D(E) \equiv |S_{LR}|^2 = |S_{RL}|^2$. For the average electrical current $I = I_L = -I_R$ we have from Eq.(2.22)

$$I = \frac{e}{h} \int dE\, D(E)\, [f_L(E) - f_R(E)]\,, \tag{2.36}$$

which in the linear response regime reduces to

$$I = -V \frac{e^2}{h} \int dE\, \frac{df(E)}{dE} D(E), \tag{2.37}$$

as discussed above.

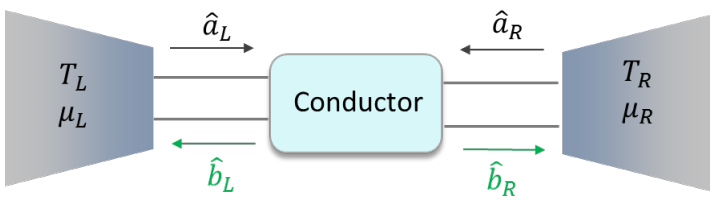

Figure 2.2: Schematic of mesoscopic conductor coupled to $N = 2$ terminals, left (L) and right (R). The quantities $T_\alpha, \mu_\alpha, \hat{a}_\alpha$ and $\hat{b}_\alpha$, with $\alpha = L, R$ are explained in Fig. 2.1

For the current correlations we have $P = P_{RR} = P_{LL} = -P_{LR} = -P_{RL}$, given from Eq.(2.32) to be

$$P = \frac{e^2}{h} \int_{-\infty}^{\infty} dE \Big\{ D(E)[f_L(E)(1 - f_L(E)) + f_R(E)(1 - f_R(E))] \\ + D(E)[1 - D(E)][f_L(E) - f_R(E)]^2 \Big\}. \tag{2.38}$$

From this expression it is clear that at zero temperature, $T = 0$, the equilibrium part of the noise, i.e. the term proportional to $f_L(E)[1 - f_L(E)] + f_R(E)[1 - f_R(E)]$, goes to zero. The noise is then given by the second, shot noise, term proportional to $[f_L(E) -$

$f_R(E)]^2$. Considering for simplicity the case where the transmission probability $D(E) \approx D$, is independent of energy on the scale of the applied voltage, the noise becomes

$$P = \frac{e^3}{h}|V|D(1-D). \tag{2.39}$$

This expression clearly shows the probabilistic, quantum scattering nature of the shot noise. For $D = 0$, there is no current flowing and hence the noise is zero. For $D = 1$ there is a filled stream of electrons flowing through the completely transparent contact, without any scattering, and the noise is again zero. For $D = 1/2$, the probability to scatter is one half, and the noise is maximized.

When discussing the two-terminal conductor it is also convenient to introduce the Fano factor F, defined as

$$F = \frac{P}{eI}\,. \tag{2.40}$$

A Fano factor $F = 1$ means that the noise $P = eI$, which is known as Poisson noise, with particles transmitting across the conductor is a completely uncorrelated fashion. A Fano factor $F < 1$ implies a sub-Poissonian noise, and is a signature of anti-bunching of the transmitted particles. If the Fano factor $F > 1$ the noise is super-Poissonian and the particles tend to bunch.

The Fano factor is particularly relevant to consider for the shot noise, i.e. the zero temperature limit. Inserting the expressions for the noise in Eq.(2.39) and the current in Eq.(2.37) we have (for $V > 0$)

$$F = 1 - D. \tag{2.41}$$

Clearly, for a small transmission, $D \ll 1$, the Fano factor $F = 1$, i.e. we have uncorrelated, Poissonian, electron transfer. For any larger $D \leq 1$, we have $F < 1$, that is, the electrons tend to transmit across the conductor in an anti-bunched fashion, one by one after each other. This is a direct consequence of the Pauli exclusion principle.

2.4 Nonlinear transport and Gauge invariance

An important aspect of quantum transport in mesoscopic systems that is sometimes overlooked, is that the scattering matrix typically depends on the applied voltages and temperatures at the reservoirs, that is

$$S = S(\{V_\alpha\}, \{T_\alpha\}), \tag{2.42}$$

where $\{V_\alpha\} = V_1, V_2, V_3, ...$ and $\{T_\alpha\} = T_1, T_2, T_3, ...$ The reason for this dependence can be understood in the following way, using mean-field arguments: due to the applied voltages and temperatures, excess electrons are injected into the conductor. This excess charge is screened, by a change of the scattering potential in the conductor and by charges accumulating at nearby metallic gates and terminals. As a consequence of the changed scattering potential, the scattering matrix is changed, in a way which thus depends on applied voltages and temperatures [33, 34].

This modification of the scattering matrix is not only a small effect that in most cases can be neglected, on the contrary it is of fundamental nature, being a consequence of gauge invariance. Gauge invariance in mesoscopic systems means that if all electric potentials at the reservoirs and nearby metallic gates are simultaneously shifted by the same amount the physics should remain the same, i.e. be invariant. As a consequence, physical quantities like the current or noise, can only depend on differences between voltages applied at different reservoirs and gates.

In general, to calculate the scattering potentials induced by the applied voltages and temperatures bias and from that new scattering potential calculate the new scattering matrix is typically a very difficult, if not impossible, task. In this thesis, in papers III and IV, this is only done by making simplifying assumptions about the conductor.

Importantly, when the transport is in the linear response regime, with small applied voltages and temperatures, one can neglect the voltage and temperature dependence of the scattering matrix and the gauge invariance is always fulfilled. Formally, this is a consequence of that one expands the transport quantities to first order (linear response) in voltage and temperature bias and hence considers the scattering matrix at equilibrium. However, in the non-linear transport regime, the bias dependence of the scattering matrix becomes important and one must always assure that gauge invariance holds.

Chapter 3

Time-dependent scattering theory, Floquet approach

In the previous chapter we presented the scattering theory for time-independent mesoscopic conductors. Here we will extend this theory to describe situations where the central conductor in Fig. 2.1 is subjected to a time dependent modulation, giving rise to a periodic-in-time modulation of the scattering potential. Such a time-periodic drive is the central ingredient in a number of important physical phenomena in mesoscopic conductors, such as photon-assisted tunnelling [35, 36], adiabatic quantum pumping [27, 37, 38] and periodic on-demand emission from single particle sources [10, 11]. The latter case is the topic of Chapter 5.

We will base our approach on the Floquet scattering theory, following largely the works in Refs. [27, 39]. Quite generally, Floquet theory is an approach to treat certain problems with a periodic time-dependence of some parameter. It is often discussed as a time domain analog of Bloch's theorem in solid state physics. Floquet scattering theory for quantum transport provides a natural extension of the time-independent scattering theory discussed in the previous chapter. This is the case since the time-dependent scattering potential not only leads to transmission and reflection of electrons between different leads of the multi-terminal conductor, but also absorption and emission of one or more quanta of energy $\hbar\Omega$ by the scatterer, where Ω is the frequency of the drive. Hence, while the time-independent scattering is elastic, i.e. energy conserving, scattering from a time-dependent potential is inelastic, i.e. energy is not conserved. This inelastic scattering is illustrated in Fig. 3.1.

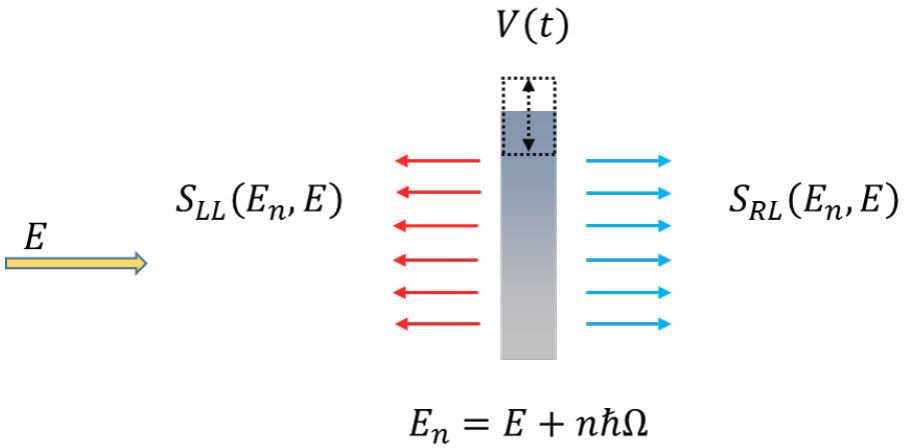

Figure 3.1: Figure showing scattering in real and energy space from a mesoscopic conductor subjected to a time-dependent potential $V(t)$ with a drive frequency Ω. An electron at energy E, incident on the scatterer from left, has an amplitude $S_{\mathrm{LL}}(E_n, E)$ to be reflected (red arrows) and an amplitude $S_{\mathrm{RL}}(E_n, E)$ to be transmitted (blue arrows) to an energy $E_n = n\hbar\Omega$. For $n > 0$ ($n < 0$) the electron thus absorbs (emits) n quanta $\hbar\Omega$ at the scattering.

Another important aspect is that a dynamic scatterer not only generates currents with an alternating component, that is AC-currents, but under some conditions can generate a DC-current. This is the case for adiabatic quantum pumps, where a DC-current is generated by (at least) two, slow, out-of-phase driving potentials, in the absence of any bias applied between the reservoirs. In a Floquet picture, the origin of this pumping effect is that the probability for particles scattering from one reservoir to another, between two energies, is different from the probability for the time-reversed process. For the time independent case, there is no corresponding phenomenon.

3.1 Floquet scattering matrix

The central quantity of the scattering theory is the Floquet scattering matrix S_F. In correspondence to the time independent case, the matrix S_F is formally obtained by solving the time-dependent Schrödinger equation for the scattering region, which typically is highly non-trivial. Here we will however express all studied transport quantities in terms of elements of S_F; only in a few cases an explicit expression of the full Floquet scattering matrix will be presented. To simplify our discussion we will consider a multi-terminal conductor with all leads supporting only a single mode.

Proceeding along the same lines as for the time-independent case, the starting point of the calculation of the transport quantities is the field operator for an electron in lead α, given

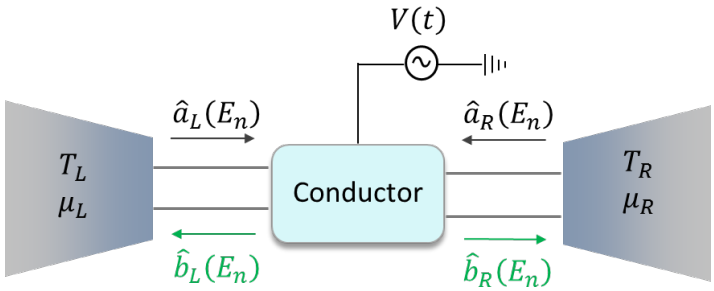

Figure 3.2: Schematic of time driven mesoscopic scatterer coupled to two terminals, left (L) and right (R). The setup, except the drive, is the same as in the time-independent case in Fig. 2.2

by Eq. (2.15). From the field operator, we hence again get the electrical current operator in Eq. (2.18), expressed in terms of operators for the outgoing, $\hat{b}^\dagger_\alpha(E), \hat{b}_\alpha(E)$, and incoming, $\hat{a}^\dagger_\alpha(E), \hat{a}_\alpha(E)$, particles. However, in contrast to the time-independent case, the operators for out- and ingoing particles are now related via the elements of the Floquet scattering matrix as

$$\hat{b}_\alpha(E_n) = \sum_m \sum_\alpha S_{F,\alpha\beta}(E_n, E_m)\hat{a}_\beta(E_m), \tag{3.1}$$

where we have introduced the notation $E_n = E + n\hbar\Omega$. The Floquet scattering matrix element $S_{F,\alpha\beta}(E_n, E_m)$ thus gives the amplitude to scatter from an energy E_m in lead β to an energy E_n in lead α, see Fig. 3.2 for a two-terminal set-up.
In contrast to the scattering matrix S for time-independent systems, the Floquet scattering matrix is infinite dimensional, due to the possibility to scatter from, in principle, one energy to any other energy differing by $(n - m)\hbar\Omega$. However, in practice, the probability to absorb or emit a large number of quanta, that is $|n - m| \gg 1$ is small. This is typically used to introduce a maximum number of quanta, $n_{\max}$, absorbed or emitted, than one needs to account for. The number $n_{\max}$ depends on the specific properties of the scattering potential and drive. However, the infinite dimensionality of S_F is thus normally not a practical problem in numerical implementations.

Importantly, as a consequence of particle current conservation during scattering, the Floquet scattering matrix is unitary [39, 40], that is

$$S_F^\dagger S_F = S_F S_F^\dagger = 1. \tag{3.2}$$

On the level of the elements, one can write this as

$$\sum_n \sum_\beta S_{F,\alpha\beta}(E_m, E_n) S^*_{F,\gamma\beta}(E_k, E_n) = \delta_{mk}\delta_{\alpha\gamma}, \tag{3.3}$$

used at several places in the discussion below.

3.1.1 Scattering matrix representations

The Floquet scattering matrix, giving the current amplitudes for scattering between different reservoirs and energies, is only one way to represent the scattering from a time-dependent potential. The three other ways, used at various places in the litterature, are the time, $S_{\alpha\beta}(t,t')$, and mixed time-energy representations $S_{\alpha\beta}(t,E_m)$, $S_{\alpha\beta}(E_n,t')$. The four different forms are related to each other via Fourier transforms, as for instance

$$S_{F,\alpha\beta}(E_n,E_m)=\frac{1}{\mathcal{T}}\int_0^{\mathcal{T}}dt\,e^{in\Omega t}S_{\alpha\beta}(t,E_m)=\frac{1}{\mathcal{T}}\int_0^{\mathcal{T}}dt\,e^{im\Omega t'}S_{\alpha\beta}(E_n,t'), \tag{3.4}$$

where $\mathcal{T}=2\pi/\Omega$ is the period of the time-dependent potential applied to the conductor. The notation convention for the mixed energy-time representation is that $S_{\alpha\beta}(t,E_m)$ gives the amplitude for a particle incident at energy E_m, from terminal β, to be scattered out at time t, to terminal α. The opposite then holds for $S_{\alpha\beta}(E_m,t)$. As is discussed further below, the mixed forms are convenient in particular for discussions in the adiabatic limit, as is the case in paper II.

3.1.2 Electrical current

Proceeding in the same way as for the time-independent case to evaluate the (quantum statistical) average $\langle I_\alpha(t)\rangle$ of the electrical current in a lead α, we make use of the pairing relations in Eq. (2.19). This directly gives the average current

$$\langle I_\alpha(t)\rangle=\sum_{n=-\infty}^{\infty}e^{in\Omega t}I_\alpha^{(n)}, \tag{3.5}$$

a sum of the DC-term $I_\alpha^{(0)}$ and the AC-terms $I_\alpha^{(n)}$, $n\neq 0$, given by the general expression

$$I_\alpha^{(n)}=\frac{e}{h}\int dE\sum_m\sum_\beta S^*_{F,\alpha\beta}(E,E_m)S_{F,\alpha\beta}(E_n,E_m)\left[f_\beta(E_m)-f_\alpha(E)\right]. \tag{3.6}$$

We note that $I^{(n)}=[I^{(-n)}]^*$, guaranteeing that the current $\langle I_\alpha(t)\rangle$ is a real quantity. Focusing on the DC-current, we have, explicitly

$$I_\alpha^{(0)}=\frac{e}{h}\int dE\sum_m\sum_\beta |S_{F,\alpha\beta}(E,E_m)|^2\left[f_\beta(E_m)-f_\alpha(E)\right]. \tag{3.7}$$

Clearly, in the absence of time-dependent drive no energy quanta can be absorbed or emitted and the Floquet scattering matrix element $S_{F,\alpha\beta}(E,E_m)=S_{\alpha\beta}(E)\delta_{m0}$, with $S_{\alpha\beta}(E)$ the time-independent scattering amplitude. As a consequence, the current in Eq. (3.7) reduces

to the time-independent expression in Eq. (2.22). The current expression in Eq. (3.7) also demonstrates that for $S_{F,\alpha\beta}(E_n, E) \neq S_{F,\alpha\beta}(E, E_n)$, a DC-current will be generated even if all terminals are kept at the same potential, that is $f_\alpha(E) = f(E)$ for all α, as discussed above. The DC-current expression in Eq. (3.7) is used at various places in papers II and IV.

3.2 Adiabatic regime

A particularly interesting case of time-dependent scattering is when the drive is very slow, called the adiabatic regime. In the adiabatic regime it is possible to relate the Floquet scattering matrix elements to the corresponding time-independent scattering matrix elements, with the scattering potential evaluated at a given, fixed, time t (time thus entering only as a parameter). This scattering matrix is known as the *frozen scattering matrix*, denoted $S^{(0)}(E, t)$. This relation constitutes a considerable simplification of calculating the Floquet scattering matrix, which in the general case has to be obtained from the solution of the time-dependent Schrödinger equation, as discussed above.

One definition of the adiabatic regime is when the energy related to the driving frequency, $\hbar\Omega$, is much smaller than the typical energy scale ΔE over which the frozen scattering matrix of varies (for all times t). Appealing to the relation between the scattering dwell time and the energy variation of the scattering matrix, one can describe the adiabatic regime as follows: during the time the electron spends inside the scattering region, the time-dependent drive potential does not change appreciably, that is, the electron sees a practically frozen scattering potential. This enables one to write the frozen scattering matrix elements in terms of the elements of the mixed energy-time representations of the scattering matrix introduced above, as

$$S^{(0)}_{\alpha\beta}(t, E) = S_{\alpha\beta}(t, E) = S_{\alpha\beta}(E, t). \tag{3.8}$$

Here, the first equality tells that the frozen scattering matrix is equal to the scattering matrix describing particles injected at energy E and emitted at time t, taken in the adiabatic regime. The second equality tells that, in the adiabatic regime, this is the same as the scattering matrix describing particles injected at time t and emitted with an energy E, consistent with the discussion above. A formal derivation of this can be found in Ref. [39].

From Eq. (3.8) and the general relation between the Floquet matrix elements and the mixed time-energy representation matrix in Eq. (3.4), we can then write

$$S_{F,\alpha\beta}(E_n, E) = \frac{1}{\mathcal{T}} \int_0^{\mathcal{T}} dt\, e^{-in\Omega t} S^{(0)}_{\alpha\beta}(t, E). \tag{3.9}$$

We note that the Floquet scattering amplitude in the adiabatic regime, in line with the discussion above, only depends on the energy E and the number of quanta n emitted or

absorbed, and thus not on the incoming and outgoing energies separately. We will present examples of this in Chapter 5, where the Floquet scattering approach is applied to the time-driven mesoscopic capacitor.

3.3 Low frequency noise

Just as for the time-dependent scattering theory, it is interesting to analyze not only the average current but also the noise in the case with periodic driving. The starting point is very similar to Eq. (2.26) for the correlation function of the current, with the difference that the correlation function now depends on two times, that is, we can write

$$P_{\alpha\beta}(t,t') \equiv \left[\frac{1}{2}\langle \Delta\hat{I}_\alpha(t)\Delta\hat{I}_\beta(t') + \Delta\hat{I}_\beta(t)\Delta\hat{I}_\alpha(t')\rangle\right]. \tag{3.10}$$

As for the time-independent case, we are mainly interested in the zero frequency noise, which is defined as

$$P_{\alpha\beta}(\tau) = \int_{-\infty}^{\infty} dt'' P_{\alpha\beta}(\tau + t''/2, \tau - t''/2), \tag{3.11}$$

where $\tau = \frac{t+t'}{2}$ and the integration is performed over the time difference $t - t' = t''$. Similar to the average, time-dependent current, we can write the average, time-dependent, zero frequency noise as

$$P_{\alpha\beta}(\tau) = \sum_{n=-\infty}^{\infty} e^{in\Omega t} P^{(n)}_{\alpha\beta}, \tag{3.12}$$

a sum of a DC noise term $P^{(0)}_{\alpha\beta}$ and AC noise terms $P^{(n)}_{\alpha\beta}$, $n \neq 0$. To be explicit, the DC term, which is the one we will discuss further here, is often written as the period averaged noise,

$$P_{\alpha\beta} \equiv P^{(0)}_{\alpha\beta} = \int_0^{\mathcal{T}} \frac{d\tau}{\mathcal{T}} P_{\alpha\beta}(\tau). \tag{3.13}$$

The general expression for the zero frequency, period averaged noise is quite lengthy and here we only discuss the case where all terminals are kept at the same electrical potential. The noise is then given by

$$P_{\alpha\beta} = \frac{e^2}{h}\int_0^{\infty} dE \left[P^{\text{th}}_{\alpha\beta}(E) + P^{\text{sh}}_{\alpha\beta}(E)\right], \tag{3.14}$$

where $P^{\text{th}}_{\alpha\beta}(E)$ and $P^{\text{sh}}_{\alpha\beta}(E)$ are the spectral thermal noise and shot noise contributions respectively, defined as,

$$P^{\text{th}}_{\alpha\beta}(E) = f(E)\,[1-f(E)]\left(\delta_{\alpha\beta} + \sum_{n=-\infty}^{\infty}\left[\delta_{\alpha\beta}\sum_{\gamma}|S_{F,\alpha\gamma}(E_n,E)|^2 - |S_{F,\alpha\beta}(E_n,E)|^2 - |S_{F,\beta\alpha}(E_n,E)|^2\right]\right), \tag{3.15}$$

and

$$P^{\text{sh}}_{\alpha\beta}(E) = \sum_{\gamma,\delta}\sum_{n=-\infty}^{\infty}\sum_{m=-\infty}^{\infty}\sum_{p=-\infty}^{\infty}\frac{[f(E_n)-f(E_m)]^2}{2} \times S^*_{F,\alpha\gamma}(E,E_n)S_{F,\alpha\delta}(E,E_m)S^*_{F,\beta\delta}(E_p,E_m)S_{F,\beta\gamma}(E_p,E_n). \tag{3.16}$$

For the thermal part, we see that it goes to zero when the temperature goes to zero, due to the term $f(E)[1-f(E)] = -k_B T df(E)/dE$. Moreover, in the absence of the time-dependent drive, when $S_{F,\alpha\beta}(E,E_m) = S_{\alpha\beta}(E)\delta_{m0}$, with $S_{\alpha\beta}(E)$ the time-independent scattering amplitude, we recover the expression in Eq. (2.33), i.e., the thermal noise for the time-independent case.

As seen from Eq. (3.16) the shot noise has the same structure, with a product of four scattering amplitudes, as the time independent shot noise in Eq. (2.39). Consequently, the origin of the noise is the same, namely the probabilistic scattering of particles. However, in the absence of a time-dependent drive, the shot noise term vanishes, which is to be expected since neither a periodic drive nor a potential bias is applied.

3.3.1 Noise in the adiabatic regime

In the adiabatic regime, the connection between the noise in the time dependent and time independent cases becomes even more explicit. Focusing on the thermal noise term, we can make use of the relation in Eq. (3.9) and write the expression in Eq. (3.15) as

$$P^{\text{th}}_{\alpha\beta}(E) = k_B T\left(-\frac{\partial f}{\partial E}\right)\left[2\delta_{\alpha\beta} - \overline{|S_{\alpha\beta}(E)|^2}, -\overline{|S_{\beta\alpha}(E)|^2}\right], \tag{3.17}$$

where we have introduced

$$\overline{|S_{\alpha\beta}(E)|^2} = \int_0^{\mathcal{T}}\frac{dt}{\mathcal{T}}|S^{(0)}_{\alpha\beta}(E,t)|^2, \tag{3.18}$$

the time average of the modulus square of the frozen scattering matrix element. This form is just the same as in Eq. (2.33), with the only difference that the modulus square of the time-independent scattering matrix element is replaced by the time integral over the modulus square of the frozen scattering matrix element.

Chapter 4

Thermoelectric effects and heat engines, a scattering approach

To achieve a sustainable energy production, conversion, transportation and storage is arguably one of the biggest challenges for the society in the twenty-first century. Another grand energy challenge is to evacuate heat produced in electronic devices, a problem increasing with the ongoing miniaturization and close-packing of electronic components. One part of the solution to both these challenges might be thermoelectric systems, where waste heat is converted to useful electric energy. Thermoelectric solid-state systems have been investigated since the nineteenth century, with varying intensity and progress. From the early 1990's a large effort has been made in investigating thermoelectric effects in nanoscale systems [41–43]. Here the hope has been to benefit from typical nanophysics properties, such as low-dimensionality of systems and sharply energy dependent transport properties. Despite large progress during the last decades it is fair to say that there is still a broad scope for fundamental investigations of proof-of-principle nanoscale thermoelectric systems. This has motivated a large part of the work in this thesis.

In recent years there has also been an increasing interest in investigating the possibilities for using fundamental quantum mechanical properties, such as coherence and entanglement in thermoelectric systems and devices, to achieve an advantage over their classical counterparts [9, 44]. These efforts combine knowledge and theoretical tools from the fields of quantum thermodynamics and quantum technology and are largely focused on identifying fundamental physics mechanisms as well as proposing and performing proof-of-concept experiments. The work presented in this thesis is in this spirit, we investigate combined energy and charge transport in quantum coherent, mesoscopic systems with thermoelectric properties, with the main aim to identify and analysis novel mechanisms for heat-to-electrical work conversion, as presented in papers I and II, or to explore novel phenomena arising

when combining driven and thermoelectric quantum systems, as in paper IV.

4.1 Thermoelectric laws and concepts

The field of Thermoelectrics has a long history, with important contributions already in the 19th century. For the understanding of nanoscale and quantum thermoelectric phenomena, it is helpful to first review some central, classical thermoelectric concepts. The most basic thermoelectric phenomena are the Seebeck and Peltier effects, which can be seen as each others reciprocals [45]. Using a language in line with our global, scattering approach taken in the thesis, the Seebeck effect describes an electrical voltage appearing across a conductor as a result of a temperature difference applied between the ends of the conductor while the Peltier effect describes the heat current flow through a conductor as a result of an electrical current sent through the conductor. The underlying property of the conductor, causing both effects, is that the transport is dependent on energy, on the scale of the applied temperature or voltage difference.

Qualitatively, discussing here the linear transport regime for a two-terminal conductor (providing more formal definitions below), the Seebeck effect leads to a relation between the applied temperature difference ΔT and the induced potential V as

$$V = -S\Delta T, \tag{4.1}$$

where S is the Seebeck coefficient, also called the thermopower. In conductors where the energy dependence of the transport properties is weak around Fermi energy μ, as is typically the case in metals, the Seebeck coefficient is given by Motts's law

$$S = e\mathcal{L}T\frac{d\ln G(\mu)}{d\mu}, \quad \mathcal{L} = \frac{(\pi k_B)^2}{3e^2}, \tag{4.2}$$

where G is the electrical conductance of the conductor and $\mathcal{L}$ the so-called Lorenz number. The Peltier effect leads to a relation between the electrical current I and heat current J as

$$J = \Pi I, \tag{4.3}$$

where Π is the Peltier coefficient. In the absence of a magnetic field, the relation $\Pi = TS$ holds, where T is the system temperature, as discussed further below.

In addition to the thermoelectric Seebeck and Peltier effects, to get a complete picture of the coupled charge and energy transport, we also need to consider the electric and thermal conductances. The electrical conductance G was discussed in Chapter 2. The thermal conductance κ is defined analogously to the electrical conductance; it relates the heat current

flowing through the conductor, as a result of a temperature difference between the two ends of the conductor, that is

$$J = \kappa \Delta T. \tag{4.4}$$

In conductors with weakly energy dependent transport properties the thermal and electrical conductances are directly related as

$$\kappa = \mathcal{L} T G, \tag{4.5}$$

known as the Wiedemann-Franz law.

A convenient and general formulation, capturing all linear response relations between charge, I, and heat, J, currents and the applied voltage V and temperature difference ΔT, is given in the matrix form

$$\begin{pmatrix} I \\ J \end{pmatrix} = \begin{pmatrix} G & GS \\ \Pi G & \kappa + G\Pi S \end{pmatrix} \begin{pmatrix} V \\ \Delta T \end{pmatrix}. \tag{4.6}$$

The formal definitions of the transport coefficients are

$$G = \left.\frac{I}{V}\right|_{\Delta T=0}, \quad S = -\left.\frac{V}{\Delta T}\right|_{I=0}, \quad \Pi = \left.\frac{J}{I}\right|_{\Delta T=0}, \quad \kappa = \left.\frac{J}{\Delta T}\right|_{I=0}. \tag{4.7}$$

We note that the coefficient matrix in Eq. (4.6) is very similar to the Onsager matrix [46], where I and J instead are related to V/T and $\Delta T/T^2$. Fundamental arguments shows that, in the absence of a magnetic field the Onsager matrix is symmetric, directly giving the relation $S = \Pi/T$. However in the presence of a magnetic field B, it holds as $S(B) = \Pi(-B)/T$. Moreover in the nonlinear transport regime the Onsager relations are not expected to hold anymore. For our purposes in this thesis, however, the matrix formulation in Eq. (4.6) is more useful than the Onsager matrix formulation. We note that various aspects of the breakdown of Onsagers relations in mesoscopic thermoelectrics have been investigated in a number of recent theory works [25, 47–49].

4.2 Charge and energy currents in the scattering approach

In this thesis we discuss the thermoelectric transport phenomena within a scattering picture. We follow largely the steps of Butcher [50], who provided a thorough extension of the scattering theory for charge transport (presented in Chapter 2) to also comprise energy and heat currents. First, a general, multi-terminal description is given, thereafter a more detailed discussion is presented, focusing on the conceptually simpler two-terminal case. The two-terminal case also allows for a direct comparison to the results presented in the previous section. For simplicity we assume single mode leads, an extension to multi-mode leads can be done along the same lines as for the charge current.

The quantum mechanical expression for the energy current can formally be derived along the same line as the charge current, following similar steps as in Chapter 2. Here we, however, present only the final expression in terms of scattering matrix amplitudes and reservoirs Fermi distribution functions. We consider the multi-terminal conductor in Fig. 2.1 and recall that the electrochemical potential and temperature of reservoir α are given by $\mu_\alpha = \mu + eV_\alpha$ and $T_\alpha = T + \Delta T_\alpha$ respectively. For clarity, we write both the charge, I, and energy, I^E, currents in the same equation, as

$$\begin{aligned} I_\alpha &= \frac{e}{h}\int dE \sum_\beta |S_{\alpha\beta}(E)|^2 \left[f_\beta(E) - f_\alpha(E)\right], \\ I^E_\alpha &= \frac{1}{h}\int dE\, E \sum_\beta |S_{\alpha\beta}(E)|^2 \left[f_\beta(E) - f_\alpha(E)\right]. \end{aligned} \tag{4.8}$$

From the energy and charge currents, the heat current flowing into/out from reservoir α is given by

$$J_\alpha = I^E_\alpha - \mu_\alpha I_\alpha. \tag{4.9}$$

We note that the heat current, outside linear response, is typically not conserved in the system, in contrast to the charge and energy currents. These current equations form the basis for the calculations and discussions presented in the rest of the chapter.

4.2.1 Linear response, two terminal case

In order to acquire a deeper understanding of the above results, we focus on a two-terminal system, $\alpha = L, R$, as shown in Fig. 2.2. We consider the energy and charge currents in the linear response regime and also define the charge current $I = I_R = -I_L$ and the heat current $J = J_R = -J_L$, conserved in the linear response regime.

Formally, in the linear response regime we expand the Fermi distribution functions to first order in applied voltage V_α and temperature ΔT_α as

$$\begin{aligned} f_\alpha(E) &\approx f(E) + V_\alpha \left.\frac{\partial f_\alpha(E)}{\partial V_\alpha}\right|_{\{V_\alpha,\Delta T_\alpha\}=0} + \Delta T_\alpha \left.\frac{\partial f_\alpha(E)}{\partial T_\alpha}\right|_{\{V_\alpha,\Delta T_\alpha\}=0}, \\ &= f(E) - eV_\alpha \frac{df(E)}{dE} - (E-\mu)\frac{\Delta T_\alpha}{T}\frac{df(E)}{dE}. \end{aligned} \tag{4.10}$$

We chose, without loss of generality, to define $V = V_R - V_L$ and $\Delta T = \Delta T_R, \Delta T_L = 0$. Moreover, for a two-terminal conductor the only property of the scattering matrix that enters the current expressions is the transmission probability $D(E) = |S_{\mathrm{LR}}(E)|^2$. With

these specifications we can write the electrical and heat currents in Eqs. (4.8) and (4.9), in a matrix form as

$$\begin{pmatrix} I \\ J \end{pmatrix} = \begin{pmatrix} G & L \\ M & K \end{pmatrix} \begin{pmatrix} V \\ \Delta T \end{pmatrix}, \tag{4.11}$$

where we have the transport coefficients

$$G = \frac{e^2}{h}\mathcal{I}_0, \quad L = \frac{M}{T} = \frac{e}{h}k_{\mathrm{B}}\mathcal{I}_1, \quad K = \frac{1}{h}(k_{\mathrm{B}}^2)\mathcal{I}_2, \tag{4.12}$$

with the integrals

$$\mathcal{I}_n = \int_{-\infty}^{\infty} dE\, D(E)\left(\frac{E}{k_{\mathrm{B}}T}\right)^n\left(-\frac{\partial f(E)}{\partial E}\right). \tag{4.13}$$

Here G is the electrical conductance, discussed above. Moreover, from these expressions we can directly relate the linear response coefficients L, M and K to the thermoelectric transport coefficients in Eq. (4.6) as

$$L = SG, \quad M = \Pi G, \quad K = \kappa + G\Pi S. \tag{4.14}$$

For the case of a weak energy dependence on the scale of applied potentials and temperatures, we can expand the transmission probability to first order in energy around Fermi energy as

$$D(E) \approx D + (E-\mu)\left.\frac{dD(E)}{dE}\right|_{E=\mu}. \tag{4.15}$$

Inserting this expansion into the expressions for the transport coefficients and keeping only leading order terms, we arrive at both the Mott's law in Eq. (4.2) and Wiedemann-Franz law in Eq. (4.5). This illustrates that the scattering theory of thermoelectric transport is consistent with existing, more macroscopic formulations.

4.3 Charge and energy current noise

In Chapter 2, not only the electrical current but also the associated noise was discussed. In the same way, when discussing the thermoelectric properties and coupled electric and energy (or heat) currents, an extension to the noise is interesting [17]. In addition to the correlator of energy currents, we also need to consider the mixed correlators, of charge and energy currents [51, 52]. Focusing on the zero frequency correlators between currents at terminals α and β, we are thus interested in the in total four combinations

$$P^{xy}_{\alpha\beta} = \frac{1}{2}\int d\tau \left\{\langle \Delta I^x_\alpha(t)\Delta I^y_\beta(t+\tau)\rangle + \Delta I^y_\beta(t+\tau)\langle \Delta I^x_\alpha(t)\rangle\right\}, \tag{4.16}$$

where x, y can denote either charge or energy. The correlators can be calculated following the same recipe as for the charge current correlators in Chapter 2. We then find, on a common form, an extension of Eq. (2.32) as

$$\begin{aligned} P^{xy}_{\alpha\beta} &= \frac{e^{\sigma_{xy}}}{h}\sum_{\gamma\delta}\int dE\, E^{(2-\sigma_{xy})}(\delta_{\alpha\gamma}\delta_{\alpha\delta} - S^*_{\alpha\gamma}S_{\alpha\delta})(\delta_{\beta\gamma}\delta_{\beta\delta} - S^*_{\beta\delta}S_{\beta\gamma}) \\ &\times \{f_\gamma(E)[1-f_\delta(E)] + f_\delta(E)[1-f_\gamma(E)]\}, \end{aligned} \tag{4.17}$$

where $\sigma_{xy} = 0$ for energy-energy, 1 for energy-charge, and 2 for charge-charge current correlators. In our works, the various types of current correlators are discussed in paper II.

4.4 Heat engines in mesoscopic systems

Besides the fundamental transport properties of thermoelectric systems, in this thesis we also investigate the possibilities to design heat engines, that is, heat to electric work conversion, based on mesoscopic conductors. In fact, both papers I and III are focused on using and tailoring the energy dependence of the transmission probability $D(E)$ to create, ideally, efficient and powerful heat engines that display as small fluctuations as possible. As discussed further below, it has in fact been shown very recently [53] that these three desirable properties of a heat engine can not be all achieved at the same time.

We start by a short background on heat engines, focusing on mesoscopic and nanoscale systems, of central importance to the thesis. We however note that also aspects of thermoelectric systems are interesting, as e.g. refrigeration, but they are not discussed in the thesis. The discussion below follows to a considerable extent Ref. [45].

A two-terminal mesosocopic thermoelectric heat engine uses the temperature difference between the two terminals to push an electrical current I against a voltage V applied across the conductor, thus producing electrical power

$$\mathcal{P} = IV. \tag{4.18}$$

In many situations, a large given output power $\mathcal{P}$ is desirable. It was shown by Whitney [54, 55] that for a single mode conductor, there is a maximal power that can be produced, given by $0.32(k_B\Delta T)^2/h$. This maximum power is obtained for a transmission probability with the shape of a step function in energy.

Another key performance criterium for the engine is how efficient the conversion is, with the efficiency η defined by

$$\eta = \frac{\mathcal{P}}{J}, \tag{4.19}$$

where J is the heat current flowing out of the hot terminal. Fundamental principles, holding for any heat engine, require that the efficiency is limited by the Carnot efficiency η_C, given by

$$\eta_C = 1 - \frac{T}{T + \Delta T}, \tag{4.20}$$

where T and $T + \delta T$ are the temperature of the cold and hot reservoir respectively. Making use of the linear response expressions for the charge and heat currents in Eq. (4.11), we can write the efficiency as

$$\eta = \frac{(GV + L\Delta T)V}{MV + K\Delta T} = \frac{(GV + GS\Delta T)V}{\Pi GV + (\kappa + G\Pi S)\Delta T}, \tag{4.21}$$

where we in the last step used the relations in Eq. (4.14). Maximizing the efficiency with respect to the voltage, also using $M = LT$ and $\Pi = ST$ gives

$$\eta_{\max} = \eta_C \frac{\sqrt{ZT+1} - 1}{\sqrt{ZT+1} + 1}, \quad ZT = \frac{L^2 T}{G(K - L^2 T/G)} = \frac{GS^2 T}{\kappa}. \tag{4.22}$$

Here we have introduced ZT, which is known as the figure of merit of the heat engine. As is clear from Eq. (4.22), a large ZT is desirable since it gives a large efficiency. A large amount of work has gone into finding materials and structures where ZT is large [41, 56], but to date few cases with a ZT above one have been demonstrated. An important reason for this is the unavoidable heat conduction via phonons, not discussed in this thesis, suppresses ZT [45].

In some situations, the desired property of the engine to be as efficient as possible, under the condition that the heat engine is operating at the maximally achievable power. It can the be shown that in the linear response the efficiency at maximum power is bound by

$$\eta_{CA} = \frac{\eta_C}{1 + (1 + \Delta T/T)^{-1/2}}, \tag{4.23}$$

typically referred to as the Curzon-Ahlborn efficiency [57–59].

4.4.1 Thermodynamic uncertainty relations

The fact that $\eta_{CA} < \eta_C$ shows that maximizing the power typically does not allow one to reach the theoretically maximal, Carnot, efficiency. Moreover, a heat engine operating at Carnot efficiency produces zero power. These observations show that there is clearly a trade-off between large efficiency and large power production. Very recently it was demonstrated theoretically that for a large class of thermoelectric heat engines, the trade-off includes not only power and efficiency, but also the fluctuations of the power output [60, 61]. In fact, the

power, efficiency and fluctuations are subjected to a joint bound, a so called thermodynamic uncertainty relation, given by [62]

$$\mathcal{P}\frac{\eta}{\eta_C-\eta}\frac{T}{\Delta_{\mathcal{P}}}\leq\frac{1}{2}. \tag{4.24}$$

Here $\Delta_{\mathcal{P}}$ are the zero frequency power fluctuations, which can be found from our analysis of electrical current noise P (discussed in Chapter 2 and above) as

$$\Delta_{\mathcal{P}}=\int d\tau\langle\Delta\mathcal{P}(t)\Delta\mathcal{P}(t+\tau)\rangle=V^2\int d\tau\langle\Delta I(t)\Delta I(t+\tau)\rangle=V^2P. \tag{4.25}$$

This result shows that a heat engine in an efficient way produces a stable and large amount of power, is not even theoretically possible.

We note that the relation in Eq. (4.24) is formally derived for systems described by Markovian master equations, which is not the case for the systems investigated in this thesis, which instead are described by scattering theory. In fact, for systems described by scattering theory, Eq. (4.24) has been shown to break down away from linear response [63]. We also emphasize that very recently it was shown that for every system described by a thermodynamic fluctuation relation, there is a corresponding uncertainty relation [64–67]. This promises to make thermodynamic uncertainty relations an important topic of research during the coming years. In paper III, the thermodynamic uncertainty relation is analyzed for a quantum point contact heat engine.

4.5 Examples of energy dependent transmission

As is clear from the discussion above in this chapter, in the scattering description, thermoelectric effects and heat engines rely on energy dependence of the transmission probability $D(E)$ (for two-terminal systems). We now explore two systems where the transmission probability is energy dependent, a Quantum Point Contact (QPC) [68, 69], discussed in the thesis mainly in papers III and IV, and a mesoscopic capacitor [70–72] in an interferometric setup, discussed in paper I.

4.5.1 Quantum point contact

The QPC is a basic building block in many mesoscopic systems. A schematic of a two-terminal QPC structure in a two-dimensional electron gas, implemented with electrostatic split gates, is shown in Fig. 4.1 (a) The QPC is typically described by a saddle point potential forming due to the bias applied at the split gates [69]. A detailed discussion of the QPC potential and how the scattering properties are derived is given in paper IV. Here,

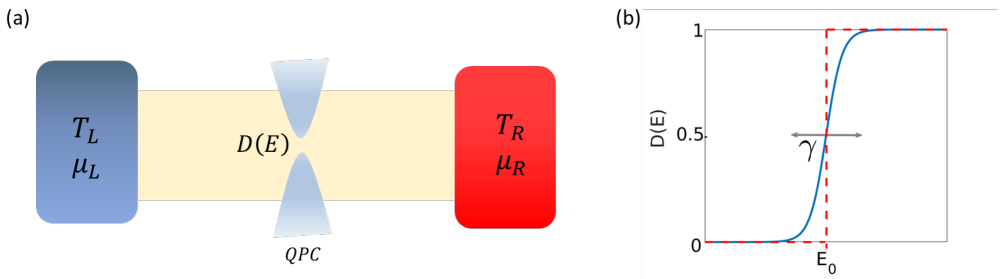

Figure 4.1: (a) Schematic of two-terminal conductor with energy dependent QPD transmission probability $D(E)$. (b) The transmission probability as a function of step energy E_0, for different smoothness γ. The smoothness is zero for the dashed red line which gives a sharp step-function transmission. By increasing γ the sharp step starts to get smoothened (blue line).

to illustrate the energy dependence of the scattering, we just give the transmission probability at the onset of the first propagating mode. As shown in several works [68, 69], the probability is given by the Fermi-function like expression

$$D(E) = \frac{1}{1 + \exp\left(\frac{-E+E_0}{\gamma}\right)}. \tag{4.26}$$

A plot of the $D(E)$ is given in Fig. 4.1 (b). The energy scale E_0 sets the position of the step in transmission from 0 to 1, with $D(E_0) = 1/2$. The energy γ gives the width in energy of the step. The step energy E_0, and to some extent also γ, are tunable via the split gate potentials. The thermoelectric and heat engine properties of the QPC is discussed in detail in paper III.

In the ideal case, to obtain maximal power, one would like to have a $\gamma \to 0$. However, this is difficult from an experimental point of view. Instead, in many situations the energy scale γ is so large that for all practical purposes one can neglect the energy dependence of $D(E)$ and just put $D(0)$, that is, the transmission probability at Fermi energy. This is the case in the next sub-section.

4.5.2 Mesoscopic capacitor in interferometer

A more elaborate scheme, built on achieving a sharp step in energy by quantum interference, is the topic of paper I. It is however helpful for the discussion in this section and the next chapter to describe the scheme in some detail. The scheme consist of two building blocks, a mesoscopic capacitor which is then inserted in an electronic Mach-Zehnder interferometer.

The mesoscopic capacitor is shown schematically in Fig. 4.2. It is implemented in a two-dimensional electron gas in the quantum Hall regime, where the transport takes place along

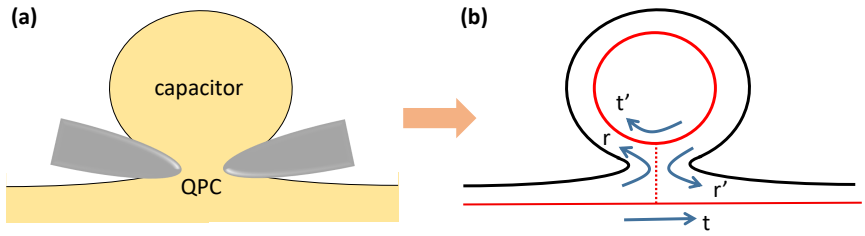

Figure 4.2: Mesoscopic capacitor and scattering amplitudes. Left panel: Schematic top-view of capacitor defined in a two-dimensional electron gas, with QPC top-gate electrodes in grey. Right panel: Scattering paths and corresponding amplitudes t, t', r, r' at QPC shown. For details of capacitor properties, see text.

chiral edge states. The capacitor consists of a dot, with a circumference of length L, coupled via a QPC with energy independent transmission probability D_{cap}, to an edge state. An electron at energy E, with wave number k, propagating along the edge has the amplitude t to pass the capacitor without entering, the amplitude $re^{ikL}r'$ to scatter into the capacitor, go one lap around and then out again continuing along the edge, etc... . The total amplitude for the electron to pass the capacitor, summing up the amplitudes for all possible paths, is thus

$$t_{\text{tot}} = t + re^{ikL}r' + re^{ikL}t'e^{ikL}r' + \ldots = t + \frac{rr'e^{ikL}}{1 - t'e^{ikL}}. \tag{4.27}$$

Importantly, after the scattering at the capacitor the electron will eventually continue its propagation along the edge, so the probability to transmit is unity, $|t_{\text{tot}}|^2 = 1$. It is thus possible to write $t_{\text{tot}} = e^{i\alpha(E)}$, where $\alpha(E)$ is an energy dependent phase. This can be seen by rewriting t_{tot}, making use of the unitarity of the QPC scattering matrix, (up to an unimportant phase factor)

$$t_{\text{tot}} = \frac{1 - \sqrt{1 - D_{\text{cap}}}e^{-i(kL+\phi)}}{1 - \sqrt{1 - D_{\text{cap}}}e^{i(kL+\phi)}} \equiv e^{i\alpha(E)}, \tag{4.28}$$

where ϕ is a scattering phase picked up by the electron when reflecting from the QPC while circulating in the capacitor. From Eq. (4.28) the phase $\alpha(E)$ is given by

$$\alpha(E) = 2\arctan\left(\frac{\sqrt{1 - D_{\text{cap}}}\sin(kL + \phi)}{1 - \sqrt{1 - D_{\text{cap}}}\cos(kL + \phi)}\right). \tag{4.29}$$

The energy dependence of $\alpha(E)$ is discussed in detail in paper I.

The second component is the electronic Mach-Zehnder interferometer[73–76]. The classical, optical Mach-Zehnder interferometer [77] is a well know system, shown schematically in Fig. 4.3 (a). A beam of light is split into two by a semi-transparent beam splitter. The two partial beams travel along different paths (typically reflected by mirrors at some point) and

are then recombined, from different directions, on a second beam splitter. After the second beam splitter, the intensity of the light is measured in a detector. The measured intensity depends on the optical path length difference for the two partial beams, a result of interference. The interferometry can be performed also with individual quanta of light, photons,

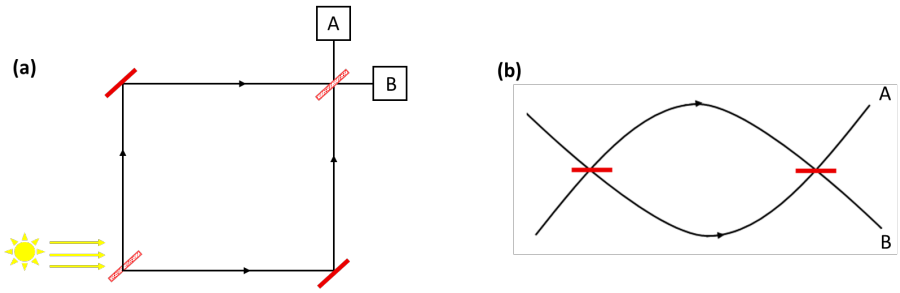

Figure 4.3: (a) Schematic of optical Mach-Zehnder interferometer with a source (sun), two semi-transparent beam splitters (speckled rectangles), two mirrors (filled rectangles), two arms and two detectors, A and B. (b) Topologically equivalent system to (a), emphasizing the two-path aspect of the interferometer. For details, see the text.

and then the Mach-Zehnder interferometer acts as a which-path (or a double-slit) interferometer for the photons. For the electronic Mach-Zehnder interferometer, the single photon interferometer is the most clear analogy. The electronic interferometers realized experimentally [73–76] are constructed in two dimensional conductors in the the quantum Hall regime, just as for the mesoscopic capacitor. In the interferometer, the electrons propagate along an edge state and scatter at two QPCs acting as beam splitters, see Fig. 4.3 (b). As dictated by quantum mechanics the total amplitude for the electron to scatter from one source terminal to a detector terminal is the sum of the amplitues for the two paths. For semi transparent QPC beam splitters, $D_{\mathrm{QPC}} = 1/2$, the amplitude can be written (up to an unimportant phase factor)

$$t_{\mathrm{MZ}} = \frac{1}{2} e^{ikL_{\mathrm{U}}} + \frac{1}{2} e^{ikL_{\mathrm{D}}} e^{i\theta}, \tag{4.30}$$

where $L\mathrm{U}$ and L_{D} are the lengths of the upper (U) and lower (D) paths in the figure. The only qualitative difference to an optical interferometer is the additional Aharonov-Bohm phase θ, proportional to magnetic flux enclosed by the two interferometer arms. Such a phase is absent for the optical interferometer since photons, in contrast to electrons, do not couple to the vector potential.

From the amplitude we have the probability

$$|t_{\mathrm{MZ}}|^2 = \frac{1 + \cos(k(L_{\mathrm{D}} - L_{\mathrm{U}}) + \theta)}{2}, \tag{4.31}$$

of the typical interference form, with a phase dependent on both the path length difference $L_{\mathrm{U}} - L_{\mathrm{D}}$, the phase θ and the energy E, via the wave number $k(E)$.

Combining the two components, by coupling a mesoscopic capacitor to the upper arm of the Mach-Zehnder interferometer, we get a total transmission amplitude

$$t_{\mathrm{MZ,tot}} = \frac{1}{2} e^{ikL_{\mathrm{U}}} + \frac{1}{2} e^{ikL_{\mathrm{D}}} e^{i[\theta+\alpha(E)]}, \tag{4.32}$$

and hence the probability

$$|t_{\mathrm{MZ,tot}}|^2 = \frac{1 + \cos[k(L_{\mathrm{D}} - L_{\mathrm{U}}) + \theta + \alpha(E)]}{2}. \tag{4.33}$$

This shows that the effect of the mesoscopic capacitor is to modify the energy dependence of the interference. As is shown in paper I, this can be used to create a very sharp-in-energy step in the total transmission and hence a heat engine producing power close to the maximum for a single mode engine.

Chapter 5

Single electron sources

In quantum optics, fast, accurate and reliable single photon sources [78, 79]are both important tools for testing fundamental properties of quantum mechanics and also key building blocks in a number of applications within quantum technology. In quantum electronics, their counterparts single electron sources, have been investigated in a number of different contexts. First, within the field of metrology, since the 1990's, single electron sources have been designed and analysed with the purpose of creating accurate standards of charge currents [11, 80]. These efforts recently contributed to the redefinition of the Ampere in the SI-system.

Second, of interest to the work in this thesis, is the creation of well controlled sources of electrons, and sometimes holes, emitted in mesoscopic conductors at energies close to the Fermi energy. The two experimentally realized sources are the driven mesoscopic capacitor, realized by Feve and coworkers in 2007 [12], and the Leviton source, realized by the team of Glattli in 2013 [13]. These sources have not been used for metrological purposes, but rather to perform fundamental experiments with electrons, both mimicking quantum optics experiments but also to propose and perform experiments with no optical counterparts. Among the electron quantum optics experiments one can mention for example the Hong-Ou-Mandel interferometer [81, 82] and the tomographic reconstruction of a single electron wave function [83]. The experimental development of the single electron sources have also spurred a lot of theory work [84–87].

In this thesis, we compare the properties of the Leviton source and the driven mesoscopic capacitor in paper II and combine a driven mesoscopic capacitor with a thermoelectric scatterer, a QPC with energy dependent scattering, in paper IV. The focus of this chapter is to provide a detailed description of the mesoscopic capacitor, based on the time dependent, Floquet, scattering theory, outlined in Chapter 3.

5.1 Time driven mesoscopic capacitor

The mesoscopic capacitor was described in detail in Chapter 4, in the case where the scattering is time independent. Here we discuss the same structure, implemented in a conductor in the quantum Hall regime, but now coupled to an additional gate that controls the potential of the capacitor, see Fig. 5.1 a). By driving the potential of the capacitor periodically in time, with period $\mathcal{T}$, electrons and holes will be emitted from the capacitor into the propagating edge states. This is illustrated in Fig. 5.1 b).

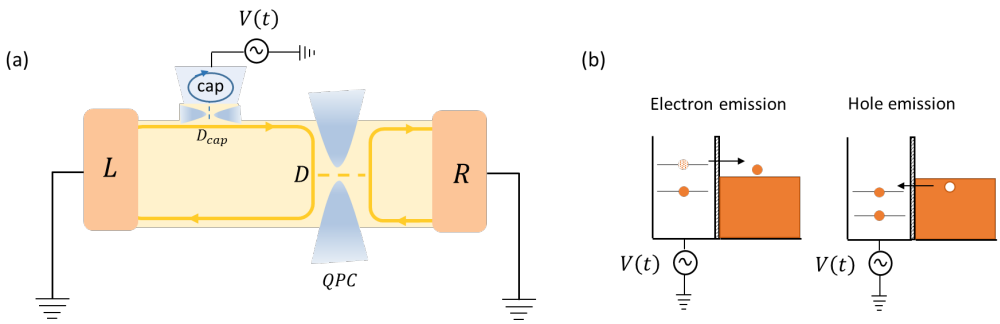

Figure 5.1: (a) Two terminal conductor in the quantum Hall regime, with a mesocopic capacitor (see Fig. 4.2.) single electron source and a QPC. The electronic reservoirs are kept at ground (no applied electric bias). Transport takes place along edge states (yellow lines). The capacitor, coupled to the edge state via a QPC with transparency D_{cap}, has its potential modulated periodically in time by an applied voltage $V(t)$, giving rise to an alternating emission of electrons and holes. The electrons and holes emitted from the capacitor scatter at the QPC, with transparency D. (b) The electron and hole emission from the capacitor, hosting a number of discrete states, is shown.

In the ideal case, considered throughout the thesis, exactly one electron and one hole will be emitted per period.

We now discuss in some detail how this qualitative picture arises from Floquet picture calculations. The starting point is the scattering amplitude for the capacitor in the mixed energy-time representation, given by [88]

$$S_{\text{cap}}(t,E) = t + rr' \sum_{q=1}^{\infty} t'^{q-1} e^{iqkL - i\phi_q(t)}, \quad \phi_q(t) = \frac{1}{\hbar}\int_{t-q\tau}^{t} dt' U(t'), \tag{5.1}$$

where E is incident energy of the electron and t is the time at which the electron leaves the capacitor. We recall from Chapter 4 that r, r', t, t' are the scattering amplitudes of the QPC defining the capacitor. In Eq. (5.1) $\phi_q(t)$ is the dynamical phase picked up during q round trips of the capacitor, with $U(t)$ the time-dependent electrical potential energy at the capacitor. Also, $\tau = L/v_F$ is the time it takes for the electron to encircle the capacitor once, with v_F the velocity at Fermi energy.

In the adiabatic regime, as discussed in chapter 2, the electron sees an essentially frozen scattering potential during the time it dwells in the capacitor. Formally, the adiabaticity criterion is

$$\Omega\tau \ll D_{\text{cap}}. \tag{5.2}$$

This corresponds to a potential (energy) $U(t)$ that is essentially constant in the time interval $[t - q\tau, t]$ and hence, we can write the phase $\phi_q(t) = q\tau U(t)/\hbar$. Inserting this into Eq. (5.1) we can perform the sum and arrive at, making use of the unitarity of the scattering matrix of the QPC (up to a constant phase factor),

$$S_{\text{cap}}(t, E) = \frac{\sqrt{1 - D_{\text{cap}}} - e^{i[kL+\theta(t)]}}{1 - \sqrt{1 - D_{\text{cap}}}e^{i[kL+\theta(t)]}}, \tag{5.3}$$

where $\theta(t) = \tau U(t)/\hbar + \phi$, with ϕ a constant scattering phase of the QPC. By comparing Eq. (5.3) to Eq. (4.28) we see that $S_{\text{cap}}(t, E)$ is indeed the frozen scattering amplitude of the capacitor.

As a next step we consider a harmonic drive potential $U(t) = \bar{U} - \delta U \sin(\Omega t)$, where Ω is the drive frequency. Moreover, linearizing the electron spectrum around Fermi energy we can write $k(E) = k_{\text{F}} + E\tau/\hbar$. Putting this into the frozen scattering matrix we have

$$S_{\text{cap}}(t, E) = \frac{\sqrt{1 - D_{\text{cap}}} - e^{i\phi(t,E)}}{1 - \sqrt{1 - D_{\text{cap}}}e^{i\phi(t,E)}}, \quad \phi(t, E) = \frac{E\tau}{\hbar} + \frac{\tau\delta U \sin(\Omega t)}{\hbar} + \phi_0, \tag{5.4}$$

where all constant phases are collected into ϕ_0.

5.1.1 Full Floquet expression

To write the corresponding scattering matrix elements in energy representation, $S^{(0)}(E_n, E)$ i.e. the Floquet matrix, we need to perform a Fourier transform of Eq. (5.4), see Chapter 3, Eq. (3.9). The transform is conveniently performed by turning it into a contour integral in the complex plane by a change of variables as $z = e^{i\Omega t}$. This gives

$$S^{(0)}(E_n, E) = \frac{1}{2\pi i}\oint dz z^{n-1} e \frac{t - e^{i\alpha}\exp\left[\frac{\beta}{2}\left(z - \frac{1}{z}\right)\right]}{1 - te^{i\alpha}\exp\left[\frac{\beta}{2}\left(z - \frac{1}{z}\right)\right]}, \tag{5.5}$$

where we introduced $\alpha = \phi_0 + E\tau/\hbar$ and $\beta = \delta U\tau/\hbar$. The integral is then given by the sum of the residues over the poles inside the complex unit circle. For $n \geq 1$, the poles are found from the roots of the denominator, and are given by

$$z_p = \kappa_p - \sqrt{1 + \kappa_p^2}, \quad \kappa_p = \frac{-[i(\alpha + 2\pi p) + \ln(t)]}{\beta}. \tag{5.6}$$

Calculating the residues then gives for the scattering matrix elements,

$$S^{(0)}(E_n, E) = \frac{2\hbar}{\delta U \tau} \frac{D_{cap}}{\sqrt{1 - D_{cap}}} \sum_{p=-\infty}^{\infty} \frac{z_p^{n-1}}{1 + 1/z_p^2}. \tag{5.7}$$

The amplitude for $n \leq 1$ is found similarly and the term for $n = 0$ can then be found from unitarity of the scattering matrix. In many situations of relevance the terms in the sum in Eq. (5.7) decay rapidly with increasing p, which makes the expression in Eq. (5.7) convenient for a numerical investigation of the scattering properties of the capacitor, for arbitrary magnitude of the QPC transmission probability D_{cap}.

5.1.2 QPC tunneling regime

In this thesis we are focusing on the case where the capacitor QPC is in the tunnelling regime, that is $D_{\text{cap}} \ll 1$. This regime can be investigated by taking the tunneling limit of the expression in Eq. (5.7). It is however more physically transparent to take this limit already for the frozen scattering amplitude in Eq. (5.4). By choosing $\bar{U}$ and δU such that there is only one electron and one hole emitted per period [18], at times $t^{(e)}(E)$ and $t^{(h)}(E)$ espectively, well separated in time, we can write the frozen scattering amplitude as a sum over amplitudes at times close to $t^{(e)}(E)$ and $t^{(h)}(E)$ as

$$S^{(0)}(t, E) = \begin{cases} \frac{t - t^{(e)}(E) + i\sigma}{t - t^{(e)}(E) - i\sigma} & -\frac{\tau}{4} < t < \frac{\tau}{4}, \\ \\ \frac{t - t^{(h)}(E) - i\sigma}{t - t^{(h)}(E) + i\sigma} & \frac{\tau}{4} < t < \frac{3\tau}{4}, \end{cases} \tag{5.8}$$

with, keeping only lowest order in energy,

$$t^{(e)}(E) = -\frac{E}{\delta U \Omega}, \quad t^{(h)}(E) = \frac{\mathcal{T}}{2} + \frac{E}{\delta U \Omega}, \quad \sigma = \frac{\hbar D_{\text{cap}}}{2\hbar\tau\delta U\Omega}. \tag{5.9}$$

This result implies that there are two emission events at (energy dependent) times $t^{(e)}(E)$ and $t^{(h)}(E)$, of temporal width σ, separated approximately half a period. Note that $\sigma \ll \mathcal{T}$, guaranteeing that the pulses are well separated.

It is instructive to reformulate the expression for the scattering amplitude in Eq. (5.8) as

$$S^{(0)}(t, E) = \frac{E - \mathcal{E}^{(e)}(t) + i\Gamma/2}{E - \mathcal{E}^{(e)}(t) - i\Gamma/2} + \frac{E - \mathcal{E}^{(h)}(t) - i\Gamma/2}{E - \mathcal{E}^{(h)}(t) + i\Gamma/2}, \tag{5.10}$$

where

$$\mathcal{E}^{(e)}(t) = \delta U \Omega t, \quad \mathcal{E}^{(h)}(t) = \delta U \Omega \left(\frac{\mathcal{T}}{2} - t \right), \quad \Gamma = \frac{\hbar D_{\text{cap}}}{\tau}. \tag{5.11}$$

This equivalent way of writing the scattering amplitude shows an emission of an electron and a hole, at energies $\mathcal{E}^{(e)}(t)$ and $\mathcal{E}^{(h)}(t)$ respectively, with spectral width $\Gamma/2$.

From Eq. (5.8) one can now calculate the Floquet matrix elements by Fourier transforming. We then get

$$S^{(0)}(E_n, E) = \begin{cases} -2\Omega\sigma e^{-n\Omega\sigma} e^{in\Omega t^{(e)}(E)} & n > 0, \\ 1 & n = 0, \\ -2\Omega\sigma e^{n\Omega\sigma} e^{in\Omega t^{(h)}(E)} & n < 0. \end{cases} \tag{5.12}$$

This is the expression which is used in papers II and IV.

Chapter 6

Summary and outlook

In this thesis two topics within mesoscopic physics have been addressed, thermoelectric transport and single electron sources. We perform a theoretical analysis of both of them individually as well as their interplay. The analysis is performed within the framework of scattering theory, which due to its conceptual simplicity allows for physically clear and compelling interpretations of the different phenomena encountered. The thermoelectric transport investigations are focused on fundamental quantum properties and proof-of-principle heat engines proposals. For the single electron sources we investigate different types of sources which emit single electrons or holes close to Fermi energy. Here we focus on the charge and energy currents and their correlators. We also analyse single electron sources operating in thermoelectrical conductors. These combined investigations reveal a number of interesting, novel phenomena and motivate both experimental as well as further theoretical studies.

In Paper I we show theoretically that a thermoelectric heat engine, with operation based only on quantum-mechanical interference, can reach optimal performance in the linear response regime. As a concrete experimental proposal, we consider a two-terminal conductor in the quantum Hall regime, where transport takes place along chiral edge states. It is shown that implementation of a close-to-optimal heat engine is possible in an electronic Mach-Zehnder interferometer with a mesoscopic capacitor coupled to one arm. We demonstrate that the maximum power and corresponding efficiency can reach 90% and 83%, respectively, of the theoretical maximum. The proposed heat engine can be realized with existing experimental techniques and has a performance robust against moderate dephasing.

In Paper II we analyze different types of time-dependently driven single-particle sources whose common feature is that they produce pulses of integer charge on top of the Fermi sea. These sources are: a slowly driven mesoscopic capacitor in the quantum Hall regime,

a Lorentzian-shaped time-dependent bias voltage, and a local gate-voltage modulation of a ballistic channel. The first two types of sources have been realized experimentally and are frequently used as building blocks in electron quantum optics experiments. We explore if and how the basic differences of the three sources impact transport properties. Specifically, we address time- and energy-resolved charge and energy currents as well as the corresponding zero-frequency current correlators. In particular, we identify differences in the impact temperature has on the observables for sources with and without energy-dependent scattering properties.

In Paper III we analyze the trade-off between large power output, high efficiency and small fluctuations in the steady state operation of a thermoelectric heat engine. We provide a concrete illustration of the trade-off by theoretically investigating a quantum point contact with an energy-dependent transmission function. To analyse different operation regimes, we allow for arbitrary smoothness of the transmission probability of the point contact, which exhibits a close to step-like dependence in energy. In particular, we consider both the linear and the non-linear regime of operation. It is found that for a broad range of parameters, the power production reaches nearly its theoretical maximum value, with efficiencies more than half of the Carnot efficiency and at the same time with rather small fluctuations. Moreover, we show that by demanding a non-zero power production, in the linear regime a thermodynamic uncertainty relation can be formulated in terms of the thermoelectric figure of merit.

In paper IV we investigate a thermoelectric mesoscopic conductor, which is voltage- and temperature-biased and additionally fed by a time-dependently driven single-particle source. The conductor is a quantum point contact with an energy dependent transmission. The focus of the investigation is the interplay between stationary biases and time-dependent driving, which results in quantum screening effects at the point contact. The effects are visible in the linear thermoelectric response coeffcients and can be tuned by the time-dependent driving. This opens up for the investigation of unexplored quantum screening effects, which in other types of devices are obscured by geometric capacitive effects. Moreover, the screening effects are related to the energetic properties of the single particle source.

Based on the performed investigations and obtained results, we see several interesting extensions. A further search for experimentally realistic thermoelectric heat engines operating in the non-linear regime and combining to largest possible extent large power, high efficiency and small output fluctuations is clearly desirable. Moreover, a broad investigation of novel, fundamental effects occurring when combining single electron sources and thermoelectric transport is also motivated by the findings of Paper IV. Finally, taking a longer time perspective, it would be interesting to analyse to what extent single electron sources or thermoelectric effects could be used as building blocks for quantum technology applications.

References

[1] S. Datta, *Electronic Transport in Mesoscopic Systems* (Cambridge University Press, Cambridge, 1995).

[2] C. Beenakker and H. van Houten, in *Semiconductor Heterostructures and Nanostructures*, Solid State Physics, Vol. 44, edited by H. Ehrenreich and D. Turnbull (Academic Press, 1991) pp. 1 – 228.

[3] B. L. Altshuler, D. Khmel'nitzkii, A. I. Larkin, and P. A. Lee, Phys. Rev. B **22**, 5142 (1980).

[4] B. J. van Wees, H. van Houten, C. W. J. Beenakker, J. G. Williamson, L. P. Kouwenhoven, D. van der Marel, and C. T. Foxon, Phys. Rev. Lett. **60**, 848 (1988).

[5] D. A. Wharam, T. J. Thornton, R. Newbury, M. Pepper, H. Ahmed, J. E. F. Frost, D. G. Hasko, D. C. Peacock, D. A. Ritchie, and G. A. C. Jones, J. Phys. Condens. Matter **21**, L209 (1988).

[6] P. A. Lee and A. D. Stone, Phys. Rev. Lett. **55**, 1622 (1985).

[7] B. L. Altshuler, JETP Lett. **41**, 530 (1985).

[8] F. Giazotto, T. T. Heikkilä, A. Luukanen, A. M. Savin, and J. P. Pekola, Rev. Mod. Phys. **78**, 217 (2006).

[9] G. Benenti, G. Casati, K. Saito, and R. S. Whitney, Phys. Rep. **694**, 1 (2017).

[10] J. P. Pekola, O.-P. Saira, V. F. Maisi, A. Kemppinen, M. Möttönen, Y. A. Pashkin, and D. V. Averin, Rev. Mod. Phys. **85**, 1421 (2013).

[11] B. Kaestner and V. Kashcheyevs, Rep. Prog. Phys. **78**, 103901 (2015).

[12] G. Fève, A. Mahé, J.-M. Berroir, T. Kontos, B. Plaçais, D. C. Glattli, A. Cavanna, B. Etienne, and Y. Jin, Science **316**, 1169 (2007).

[13] J. Dubois, T. Jullien, F. Portier, P. Roche, A. Cavanna, Y. Jin, W. Wegscheider, P. Roulleau, and D. C. Glattli, Nature **502**, 659 (2013).

[14] Y. V. Nazarov and B. Y. M., *Quantum Transport: Introduction to Nanoscience* (Cambridge university press, Cambridge, 2009).

[15] R. Landauer, IBM J. Res. Dev. **1**, 223 (1957).

[16] M. Büttiker, Phys. Rev. Lett. **57**, 1761 (1986).

[17] Y. M. Blanter and M. Büttiker, Phys. Rep. **336**, 1 (2000).

[18] M. Moskalets, P. Samuelsson, and M. Büttiker, Phys. Rev. Lett. **100**, 086601 (2008).

[19] C. W. J. Beenakker and M. Büttiker, Phys. Rev. B **46**, 1889 (1992).

[20] C. W. J. Beenakker, Rev. Mod. Phys. **69**, 731 (1997).

[21] H. Förster, P. Samuelsson, S. Pilgram, and M. Büttiker, Phys. Rev. B **75**, 035340 (2007).

[22] M. de Jong and C. Beenakker, Physica A **230**, 219 (1996).

[23] H. Förster, P. Samuelsson, and M. Büttiker, New J. Phys. **9**, 117 (2007).

[24] M. Büttiker, Phys. Rev. B **33**, 3020 (1986).

[25] J. Meair and P. Jacquod, J. Phys. Condens. Matter **25**, 082201 (2013).

[26] D. Sánchez and R. López, Phys. Rev. Lett. **110**, 026804 (2013).

[27] M. Moskalets and M. Büttiker, Phys. Rev. B **66**, 205320 (2002).

[28] M. Büttiker, Phys. Rev. Lett. **65**, 2901 (1990).

[29] M. Büttiker, Physica B **175**, 199 (1991).

[30] M. Büttiker, Phys. Rev. B **46**, 12485 (1992).

[31] G. D. Mahan, *Many-Particle Physics* (Springer US, 2000).

[32] R. Kubo, Rep. Prog. Phys. **29**, 255 (1966).

[33] M. Buttiker, J. Phys. Condens. Matter **5**, 9361 (1993).

[34] T. Christen and M. Büttiker, Europhys. Lett. **35**, 523 (1996).

[35] P. K. Tien and J. P. Gordon, Phys. Rev. **129**, 647 (1963).

[36] G. Platero and R. Aguado, Phys. Rep. **395**, 1 (72004).

[37] I. L. Aleiner and A. V. Andreev, Phys. Rev. Lett. **81**, 1286 (1998).

[38] P. W. Brouwer, Phys. Rev. B **58**, R10135 (1998).

[39] M. Moskalets, *Scattering Matrix Approach to Non-Stationary Quantum Transport* (Imperial College Press, London, 2012).

[40] M. Moskalets and M. Büttiker, Phys. Rev. B **69**, 205316 (2004).

[41] L. D. Hicks and M. S. Dresselhaus, Phys. Rev. B **47**, 16631 (1993).

[42] G. D. Mahan and J. O. Sofo, Proceedings of the National Academy of Sciences **93**, 7436 (1996).

[43] M. Dresselhaus, G. Chen, M. Tang, R. Yang, H. Lee, D. Wang, Z. Ren, J.-P. Fleurial, and P. Gogna, Advanced Materials **19**, 1043 (2007).

[44] F. Binder, L. A. Correa, C. Gogolin, J. Anders, and G. Adesso, *Thermodynamics in the Quantum Regime* (Springer, New York, 2018).

[45] G. Benenti, G. Casati, K. Saito, and R. Whitney, Phys. Rep. **694**, 1 (2017).

[46] L. Onsager, Phys. Rev. **37**, 405 (1931).

[47] B. Sothmann, R. Sánchez, and A. N. Jordan, Europhys. Lett. **107**, 47003 (2014).

[48] R. Sánchez, B. Sothmann, and A. N. Jordan, Phys. Rev. Lett. **114**, 146801 (2015).

[49] R. López and D. Sánchez, Phys. Rev. B **88**, 045129 (2013).

[50] P. N. Butcher, J. Phys. Condens. Matter **2**, 4869 (1990).

[51] F. Battista, M. Moskalets, M. Albert, and P. Samuelsson, Phys. Rev. Lett. **110**, 126602 (2013).

[52] A. Crépieux and F. Michelini, J. Phys. Condens. Matter **27**, 015302 (2014).

[53] P. Pietzonka, A. C. Barato, and U. Seifert, Phys. Rev. E **93**, 052145 (2016).

[54] R. S. Whitney, Phys. Rev. Lett. **112**, 130601 (2014).

[55] R. S. Whitney, Phys. Rev. B **91**, 115425 (2015).

[56] G. J. Snyder and E. S. Toberer, Nat. Mater. **7**, 105 (2008).

[57] F. L. Curzon and B. Ahlborn, American J. Phys. **43**, 22 (1975).

[58] C. Van den Broeck, Phys. Rev. Lett. **95**, 190602 (2005).

[59] B. Jiménez de Cisneros and A. C. Hernández, Phys. Rev. Lett. **98**, 130602 (2007).

[60] T. R. Gingrich, J. M. Horowitz, N. Perunov, and J. L. England, Phys. Rev. Lett. **116**, 120601 (2016).

[61] A. C. Barato and U. Seifert, Phys. Rev. Lett. **114**, 158101 (2015).

[62] P. Pietzonka and U. Seifert, Phys. Rev. Lett. **120**, 190602 (2018).

[63] B. K. Agarwalla and D. Segal, Phys. Rev. B **98**, 155438 (2018).

[64] Y. Hasegawa and T. Van Vu, Phys. Rev. Lett. **123**, 110602 (2019).

[65] A. M. Timpanaro, G. Guarnieri, J. Goold, and G. T. Landi, Phys. Rev. Lett. **123**, 090604 (2019).

[66] T. Van Vu and Y. Hasegawa, arXiv:1904.04111 .

[67] P. P. Potts and P. Samuelsson, arXiv:1904.04913 .

[68] H. A. Fertig and B. I. Halperin, Phys. Rev. B **36**, 7969 (1987).

[69] M. Büttiker, Phys. Rev. B **41**, 7906 (1990).

[70] M. Büttiker, H. Thomas, and A. Prêtre, Phys. Lett. A **180**, 364 (1993).

[71] A. Prêtre, H. Thomas, and M. Büttiker, Phys. Rev. B **54**, 8130 (1996).

[72] J. Gabelli, G. Fève, J.-M. Berroir, B. Plaçais, A. Cavanna, B. Etienne, Y. Jin, and D. C. Glattli, Science **313**, 499 (2006).

[73] Y. Ji, Y. Chung, D. Sprinzak, M. Heiblum, D. Mahalu, and H. Shtrikman, Nature **422**, 415 (2003).

[74] I. Neder, M. Heiblum, Y. Levinson, D. Mahalu, and V. Umansky, Phys. Rev. Lett. **96**, 016804 (2006).

[75] P. Roulleau, F. Portier, D. C. Glattli, P. Roche, A. Cavanna, G. Faini, U. Gennser, and D. Mailly, Phys. Rev. B **76**, 161309 (2007).

[76] L. V. Litvin, A. Helzel, H.-P. Tranitz, W. Wegscheider, and C. Strunk, Phys. Rev. B **81**, 205425 (2010).

[77] M. Born and E. Wolf, *Principles of Optics* (Cambridge university press, 1999).

[78] B. Lounis and M. Orrit, Rep. Prog. Phys. **68**, 1129 (2005).

[79] M. D. Eisaman, J. Fan, A. Migdall, and S. V. Polyakov, Rev. Sci. Instrum. **82**, 071101 (2011).

[80] C. Bäuerle, D. C. Glattli, T. Meunier, F. Portier, P. Roche, P. Roulleau, S. Takada, and X. Waintal, Rep. Prog. Phys. **81**, 056503 (2018).

[81] E. Bocquillon, V. Freulon, J.-M. Berroir, P. Degiovanni, B. Plaçais, A. Cavanna, Y. Jin, and G. Fève, Science **339**, 1054 (2013).

[82] V. Freulon, A. Marguerite, J.-M. Berroir, B. Plaçais, A. Cavanna, Y. Jin, and G. Fève, Nat. Commun. **6**, 6854 (2015).

[83] T. Jullien, P. Roulleau, B. Roche, A. Cavanna, A. Cavanna, Y. Jin, and D. C. Glattli, Nature **514**, 603 (2014).

[84] S. Ol'khovskaya, J. Splettstoesser, M. Moskalets, and M. Büttiker, Phys. Rev. Lett. **101**, 166802 (2008).

[85] G. Haack, M. Moskalets, and M. Büttiker, Phys. Rev. B **87**, 201302 (2013).

[86] D. Ferraro, A. Feller, A. Ghibaudo, E. Thibierge, E. Bocquillon, G. Fève, C. Grenier, and P. Degiovanni, Phys. Rev. B **88**, 205303 (2013).

[87] V. Kashcheyevs and P. Samuelsson, Phys. Rev. B **95**, 245424 (2017).

[88] M. Moskalets, P. Samuelsson, and M. Büttiker, Phys. Rev. Lett. **100**, 086601 (2008).